Department of Geomatics Engineering

The Effect of Error in Gridded Digital Elevation Models on Topographic Analysis and on the Distributed Hydrological Model TOPMODEL

(URL: http://www.geomatics.ucalgary.ca/links/GradTheses.html)

by

Lynn Diane Raaflaub

September 2002

UNIVERSITY OF
CALGARY

THE UNIVERSITY OF CALGARY

The Effect of Error in Gridded Digital Elevation Models on Topographic
Analysis and on the Distributed Hydrological Model TOPMODEL

by

Lynn Diane Raaflaub

A THESIS

SUBMITTED TO THE FACULTY OF GRADUATE STUDIES

IN PARTIAL FULFILLMENT OF THE REQUIREMENTS FOR THE

DEGREE OF MASTER OF SCIENCE

DEPARTMENT OF GEOMATICS ENGINEERING

CALGARY, ALBERTA

September, 2002

Abstract

Digital elevation models (DEMs) provide the basic information required to characterise the topographic attributes of terrain. The primary derived topographic parameters associated with DEMs are slope and aspect. Slope and aspect can be used to calculate other significant topographic parameters such as upslope area and topographic index. The topographic index, in turn, can be used by distributed hydrological models, such as TOPMODEL, to characterise the spatial distribution of terrain. Many algorithms have been developed to calculate slope, aspect and upslope area from DEMs - specifically from gridded DEMs - but little work has gone into determining the uncertainty in these parameters, or the effect of this uncertainty in further applications. The accuracy of these parameters is dependent both on the algorithm used to generate them, and on the errors associated with the DEM itself. Since it is almost impossible to model all the errors associated with a given slope, aspect or upslope area algorithm, and since a DEM is normally only provided with a single rms error, simple error propagation is not adequate to determine the error associated with the derived topographic parameters. A more rigorous method of determining the effect of DEM errors on derived topographic parameters is with statistical analysis using Monte Carlo simulation and error realisations of the DEM. In this research, a comparison of slope, aspect, upslope area, and topographic index algorithms are presented along with an examination of how errors in DEMs effect the reliability of the derived topographic parameters. The effect of errors in the derived topographic parameters on the TOPMODEL hydrological model is also examined.

Acknowledgements

For his support throughout my graduate studies, I would like to thank my supervisor Dr. Michael J. Collins. My appreciation is also extended to Dr. Caterina Valeo for her assistance with the hydrological component of my study.

Many thanks go to Rebeca Quiñonez-Piñón for her help with the calibration and implementation of TOPMODEL.

Special thanks goes to Cameron Ellum for not only his proof reading skills, but also for his friendship and encouragement.

Finally, I would like to thank my parents for understanding what it means to be a graduate student. This research would not have been possible without their love and support.

Contents

List of Tables

List of Figures

ix

Chapter 1

Introduction

Digital elevation models (DEMs) model the elevation of terrain as a function of geographic location. As such, they provide the basic information required to characterise the topographic attributes of terrain. DEMs are typically represented in two formats: contour maps, where the surface is represented by lines of constant elevation at regular intervals; or point heights, where the surface elevation is sampled on a either a regular or irregular basis. The choice of a DEM format is dependent on the application, ease of analysis and, of course, on the availability of data.

The main topographic parameters derived from DEMs are slope and aspect. Slope and aspect represent the downhill surface, in the sense that they are the magnitude and direction of the vector tangent to the downhill. While the definitions of slope and aspect are fairly straightforward, the actual calculation of these variables is not. Difficulties arise in trying to model a specific element of a terrain surface from a model of a terrain surface. Because of the problems associated with deriving slope and aspect from DEMs, many algorithms have been developed to estimate these

surface descriptions.

Topographic information such as slope and aspect can be utilised by many applications. Since the spatial routing of water over terrain is strongly dependent on the shape of the downhill surface, one such application is distributed hydrological modelling. Hydrologically, slope is an indication of the amount of gravitational energy available to drive water flow, hence it influences the rate of water flow. Aspect, which defines the slope direction, can be used to determine the direction of water flow, which is the information required to determine other hydrologically significant variables such as upslope area (Zevenbergen and Thorne, 1987). Upslope area, as the name implies, delineates the total area upslope of a given location, which is an indication of how much water can flow through the location. From a hydrological standpoint, the effectiveness of a slope and especially an aspect calculation is determined by how accurately upslope area can be resolved. Like slope and aspect, there are different algorithms available for the calculation of upslope area, which are essentially dependent on the choice of algorithm used to calculate slope and aspect.

The slope, along with the upslope area (A), can be used to calculate a parameter known as the topographic index ($\ln(A/slope)$). The topographic index reflects the spatial distribution of soil moisture, surface saturation and runoff generation processes, hence it is one of the parameters used in distributed hydrological modelling. TOPMODEL is one such distributed hydrological model that uses surface topography, in the form of the topographic index, along with soil properties to predict the distribution of soil moisture and runoff (Beven and Kirkby, 1979). It uses the assumption that the spatial distribution of the topographic index approximates the spatial distribution of the depth to the water table in a watershed. Hence any variations

in the calculation of the topographic index will effect the outcome of the model's predictions.

Variations in the output of hydrological models that use parameters derived from DEMs suffer from uncertainty not only in the models used to generate the DEMs and the derived parameters, but also in the error associated with the original data itself. DEMs are normally accompanied with an estimate of accuracy, usually in the form of a root mean square (rms) error. This error should be taken into account when deriving topographic parameters and when applying these parameters, but in most cases it is not. There have been a few studies that have looked at the effect of errors in DEMs on derived topographic parameters (Fisher, 1991b,a; Lee et al., 1992; Veregin, 1997; Holmes et al., 2000), but generally, DEMs and their derived topographic parameters are treated as exact values. This can be a very questionable practice, since error can have a dramatic impact on expected results.

If all the sources of error associated with a DEM and with the algorithms used to derive the topographic parameters were known, the propagation of error through topographic parameters and hydrological models could be done using analytical error propagation. The difficulty arises in the errors associated with the assumptions inherent to the algorithms of the topographic parameters. It is almost impossible to model all the errors associated with a given algorithm, therefore a simple error propagation is not adequate to represent the error of values derived from a DEM with associated error. The effect of error in a DEM on its derived parameters is best determined with statistical analysis using Monte Carlo stimulation and error realisations of the DEM (Veregin, 1997).

1.1 Research Objectives

The primary objective of this research is to look at exactly how model and data uncertainty affect topographic analysis and the output of distributed hydrological models, namely TOPMODEL. The effect of gridded DEM data error – in the form of both correlated and uncorrelated error – will be investigated using Monte Carlo methods. Uncorrelated error is seen as the worst case scenario, where the errors in neighbouring cells are unrelated. The more realistic correlated error, on the other hand, is smoother due to the high correlation between neighbouring error values. It is hypothesised that compared to uncorrelated error, correlated error should produce less variation in the topographic parameters and TOPMODEL output.

As mentioned above, many slope and aspect algorithms have been developed to calculate these topographic parameters from DEMs, specifically from gridded DEMs. These algorithms are generally based on neighbourhood operations. The primary difference between the algorithms is the number of neighbours drawn on to complete the calculation. Two to nine grid cells may be used. In order to investigate how model uncertainty affects topographic analysis and hydrological models, nine slope and aspect algorithms will be examined. This is in essence performing an error sensitivity analysis on the various algorithms presented. The more neighbours used the more constrained the algorithms become. Therefore, it is hypothesised that the more neighbours utilised in the algorithm the less effect error will have on the derived parameters and hence on applications that use the parameters.

1.2   Thesis Outline

To accomplish the objectives presented, this thesis has been organised in the following way:

- Chapter 2 presents a more detailed discussion of DEMs, and continues with an examination of slope, aspect and upslope area algorithms.

- Chapter 3 focuses on the distributed hydrological model TOPMODEL, describing the input parameters required and how the model works.

- Chapter 4 describes the study area and data set used along with the calibration of TOPMODEL.

- Chapter 5 deals with the experimental methodology and implementation.

- Chapter 6 presents the experimental results.

- Chapter 7 provides conclusions and recommendations.

Chapter 2

Slope, Aspect and Upslope Area

2.1 Surface Representation by Gridded Elevations

The starting point for any type of digital terrain analysis is the creation of an accurate digital elevation model. A DEM may be defined as any numeric or digital representation of the terrain elevation given as a function of geographic location. As mentioned in Chapter 1, the type of DEM that is used in a given application depends on the requirements of the application and on the availability of the DEM. With the extensive use of computers in modelling, DEMs that can be easily stored and manipulated in digital form are preferable. Discrete DEMs sampled on a regular interval, known as gridded DEMs, have these advantages, and hence are utilised in most modelling processes. Actually, there are very few algorithms used to determine topographic parameters that are based on any of the other types of terrain models – including contours, TINs or mix mode.

In gridded DEMs, elevations, z, are posted at regular intervals relative to some

datum. These regular intervals can be orientated in any direction, but usually take the form of an east-west, x, and north-south, y, representation. The distance between two points is known as the grid spacing. Usually, this distance is the same for both grid directions. The elevations in a DEM normally represent the actual height of the ground at the location where they are given. A gridded representation allows for easy access and manipulation since the elevations can be stored as a simple matrix. Another advantage to using gridded DEMs as opposed to other terrain models is that they are normally easy to obtain in digital form for a given area without the need of further manipulation. Because of their regularly gridded nature, gridded DEMs suffer from sampling problems. Terrain is usually undersampled in rough areas and oversampled in flat areas, and a balance must found between the sampling interval and other requirements. The choice of grid spacing is not normally available to the user of DEMs, therefore, when looking at DEM uncertainty the issue of possible undersampling should be considered.

Though gridded DEMs have their advantages, there are a few things that need to be taken into account when using them. The data for gridded DEMs can be gotten using a variety of techniques. These include measuring the terrain directly using land-surveying or aerial photogrammetry, or interpolating from existing DEMs. However, it is important to recognise that if a DEM of one type is generated from a DEM of another type, instead of from direct measurements, it will suffer from compounded modelling error. Regardless of how a DEM is generated, it is important to remember that what is being produced is a discrete representation of a continuous surface. In other words, even the highest quality DEM is just an approximation of the surface and not an exact representation.

Gridded DEMs are usually discussed in terms of their grid spacing. Another term that is occasionally and incorrectly interchanged with grid spacing is resolution. This terminology stems from such fields as image processing, where a grid value represents an average of an area. Similarly, a gridded DEM will only have a resolution if the elevation values are grid cell averages. However, in gridded DEMs the elevation values are almost always the actual point elevations, and consequently it is normally incorrect to use resolution in place of grid spacing. It should be noted that even though when the elevations in DEMs are point values, some topographic parameter algorithms treat them as area averages.

2.2   Pit Removal

The generation of a DEM invariably introduces a number of artificial topographic features that need to be detected and corrected. Hydrologically, the most serious of these features are pits (sink features) (O'Callaghan and Mark, 1984; Band, 1986; Jenson and Dominque, 1988), and to a lesser extent, dam features (Quinn et al., 1991). Dam features occur when the elevation values are artificially raised above the actual elevation value, while pits occur at points that do not have any neighbours with a lower elevation. While it is possible for pits to be found in topographic surfaces, especially in recently glaciated areas or in limestone areas, most pits can be considered errors since fluvial erosion processes will not normally produce such features at the scale resolved by DEMs (Band, 1986). Pits generally appear in flatter areas where even a one metre error in elevation can be enough to produce a closed depression, while on steeper slopes a higher variation would be required. Serious

errors can be produced by the existence of artificial pits in a DEM for any algorithm that depends on mapping hydrologically connected regions, such as in the calculation of upslope area.

Because of the errors that pits can introduce, their removal is an important first step when using DEMs for hydrological applications. The method used for pit removal can influence the effectiveness of other algorithms applied to the DEM. There are a variety of techniques to perform pit removal – examples of their use can be found in O'Callaghan and Mark (1984); Band (1986); Martz and de Jong (1988); Jenson and Dominque (1988); Hutchinson (1989); Fairfield and Leymarie (1991); Freeman (1991); Tribe (1992); Tarboton (1997). In the simplest method, the pits are removed manually by flagging them in a preprocessing stage. Unfortunately, this process is tedious and labour intensive, and consequently a more automated approach is preferred. The most straightforward method of automated pit removal is to numerically smooth the terrain. This method reduces the number of pits, especially shallow ones, but it also tends to oversmooth the topography, which may lead to a significant loss of information. An alternative approach to pit-removal attempts to preserve flow paths and drainage directions. These other methods primarily involve finding a pit's outflow point and directing flow out through this point. This can be accomplished by raising the elevation of the pit to that of the outflow point, or by redirecting flowlines to neighbouring cells that have defined flow directions that do not point back into the pit itself.

Several of the pit removal techniques outlined above require knowledge of the surface's aspect, and, by extension, its slope. Additionally, the calculation of upslope area also requires aspect. Like pit removal, there are several techniques to calculate

these quantities. In the following section, several of these techniques are outlined.

2.3   Slope and Aspect Algorithms

Traditionally, slope and aspect were calculated manually through the use of contour data. In this method a line tangent to the contours is drawn along with its corresponding perpendicular bisector. The slope is found by dividing the difference in height along the perpendicular bisector by the length of the perpendicular bisector. Even though this method has been used to represent the 'true' slope and aspect values of a terrain (Skidmore, 1989), it is almost impossible to obtain the same values for slope and aspect twice for any given location due to the manual calculation. It is not surprising then that other methods have been developed that depend solely on digital data and programmable algorithms.

There are many different ways in which slope and aspect can be determined from gridded DEMs. Generally, their determination is based on neighbourhood operations where calculations are made for a cell based on the values of the cells that are spatially adjacent in the grid. Some methods are better than others in representing the actual slope and aspect of the terrain, while others are more suited to hydrological analysis. As mentioned previously, slope and aspect are just the magnitude and direction of the vector tangent to the topographic surface. The goal then is to define a localised topographic surface from which localised slope and aspect values can be extracted. Differences in slope and aspect algorithms have to do with how these localised surfaces are defined. These definitions are based on the number of neighbouring points used, whether or not the centre point contributes, and whether

or not the aspect calculation will be restricted to a finite number of directions (Guth, 1995). Neighbourhood slope and aspect algorithms using two to nine points in the DEM are presented in the following subsections. This is followed by a comparison of the methods. In order to make some of the algorithms easier to understand, an eight neighbourhood subgrid is defined in Figure 2.1. A symbolic representation is presented in Figure 2.1(a), while a basis for numerical examples is presented in Figure 2.1(b). Even though grid orientation should not change how the algorithms are implemented, the top of the figures will be considered north. The nine points utilised are selected from the central points at which the values are to be established, z_{ij}, and its eight adjacent neighbours, as depicted in Figure 2.1.

(a) Symbolic representation with a grid spacing of Δd.

(b) Numeric example with a grid spacing of 25 m. Elevation values are expressed in metres.

Figure 2.1: A 3×3 DEM neighbourhood.

In all the algorithms presented, except those utilising the steepest neighbours, some form of numerical differentiation is employed. This is understandable considering the basic definition of slope: the rise over the run. In terms of a topographic surface, the rise is the elevation difference and the run is the ground distance (Eyton,

1991). This definition is an example of differentiation using finite difference calculus, where the first derivative of elevation describes the rate of change of elevation, which is the slope (Eyton, 1991; Dozier and Strahler, 1983; Horn, 1981). Together, the slope in the x direction and the slope in the y direction (the partial derivatives of z with respect to the x and y directions), define the gradient vector of the surface. The maximum slope can be determined by taking the norm of this vector,

$$slope = \sqrt{\left(\frac{\partial z}{\partial x}\right)^2 + \left(\frac{\partial z}{\partial y}\right)^2}. \tag{2.1}$$

The aspect, which is the direction of the maximum slope, is the angle between the slope defined in x and the slope defined in y, which is given by the relationship

$$aspect = \tan^{-1}\left[\frac{(\partial z/\partial x)}{(\partial z/\partial y)}\right]. \tag{2.2}$$

The difference in the slope and aspect algorithms which use Equations 2.1 and 2.2 are related to how they determine the local slope in x ($\partial z/\partial x$) and y ($\partial z/\partial y$).

The determination of the local slope in x and y is dependent on one to eight of the neighbouring grid points. As a consequence, consideration must be made for those grid points that lie on the edge of the DEM, which do not have eight neighbours. In order to make the calculations consistent across the entire DEM and to avoid edge effects, the slope and aspect values are not normally calculated at the edges. In essence, this creates slope and aspect maps that are slightly smaller then the original DEM. However, this is more preferable then the alternative of obtaining grossly erroneous edge values. Therefore, all the algorithms presented are for the grid points internal to the edge.

The following subsections outline basic slope and aspect algorithms. In order to emphasise the differences between algorithms, graphical examples are presented for the algorithms in Figures 2.2–2.9. In the local neighbourhoods illustrated, the cells used in the calculation of slope and aspect are highlighted in light blue, while the dark blue arrow depicts the resulting aspect (flow direction) from the centre cell. For comparison, the numerical values for the slope and aspect are also provided.

2.3.1   Three Neighbours

Three Point Plane (TPP)

O'Neill and Mark (1987) defined a localised topographic surface using a three point plane. This method defined a triangle using three grid points: the point for which the slope and aspect value is to be calculated, and its neighbouring points to the east and north. The choice of using the eastern and northern neighbouring grid points is arbitrary, since the DEM could be orientated in any direction. Therefore, this method could be implemented using any two non-collinear neighbours. Using the northern and eastern neighbours as depicted in Figure 2.1(a), the slope in x and y can be calculated respectively as

$$\left.\frac{\partial z}{\partial x}\right|_{i,j} = \frac{z_{i,j+1} - z_{i,j}}{\Delta d} \tag{2.3a}$$

and

$$\left.\frac{\partial z}{\partial y}\right|_{i,j} = \frac{z_{i-1,j} - z_{i,j}}{\Delta d}. \tag{2.3b}$$

From these equations, and using Equations 2.1 and 2.2, the slope and aspect values for a given grid point can be determined. A numeric illustration of this algorithm is show in Figure 2.2

$$slope = 0.305$$
$$aspect = 157°$$
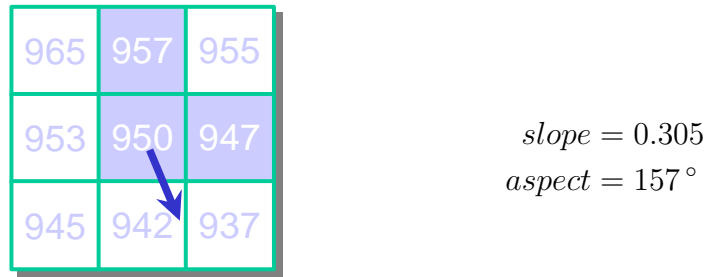
Figure 2.2: Example of the TPP method.

Four Contiguous Right Triangles

A variation of the three point plane method, in which four contiguous right triangles are used, was implemented by Onorati et al. (1992). In this method, the DEM neighbourhood is partitioned into equal, partially overlapping right triangles that are formed by connecting the centre grid point with its four nearest neighbours, i.e. those points to the north, south, east and west. A slope and aspect value is calculated for each of the four right triangles using the method described by a three point plane. The slope and aspect values calculated are attributed to the subpixel enclosed by their respective triangle. This method creates slope and aspect maps that exhibit a grid size half of that of the initial DEM. It is this rescaling effect that brings into question the accuracy of this method, and its possible use in future applications.

2.3.2 Four Neighbours

Four Closest Neighbours (FCN)

One of the more common slope and aspect algorithms uses the four closest neighbours, those to the north, south, east and west, representing a second order finite difference relationship (Hoffer et al., 1979; Unwin, 1981; Sharpnack and Akin, 1969; Ritter, 1987; Eyton, 1991; Dozier and Strahler, 1983; Skidmore, 1989; Guth, 1995; Hodgson, 1995; Jones, 1998). The elevations at these four closest neighbours can be used to define two orthogonal components of slope, the slope in x and y, which define the steepness and downhill direction, but does not define a surface at the point of interest(Guth, 1995). The orthogonal components can be calculated using the simple 'rise over run' definition of slope, which leads to the following generalised equations,

$$\left.\frac{\partial z}{\partial x}\right|_{i,j} = \frac{z_{i,j+1} - z_{i,j-1}}{2\Delta d} \tag{2.4a}$$

and

$$\left.\frac{\partial z}{\partial y}\right|_{i,j} = \frac{z_{i+1,j} - z_{i-1,j}}{2\Delta d}. \tag{2.4b}$$

Applying these equations to Equations 2.1 and 2.2, results in the determination of slope and aspect for the central point in the 3×3 neighbourhood. An illustration of the FCN algorithm is presented in Figure 2.3

$$slope = 0.323$$
$$aspect = 158\,^{\circ}$$
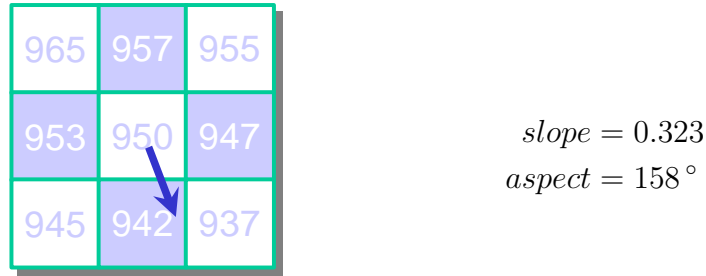
Figure 2.3: Example of the FCN method.

Four Diagonal Neighbours (FDN)

A variation to the four closest neighbours algorithm is the four diagonal neighbours algorithm (Jones, 1998). The difference in this algorithm is that the perpendicular gradients are taken at an angle of 45° to the principal axis of the DEM grid. By using the diagonal neighbours, those points to the northwest, northeast, southwest and southeast of the central point, along with a correction for the increased distance to the diagonal neighbours, allows for investigation into the possible effects of grid bias. The slope and aspect for a point can be found by solving for the slope in x and y given by,

$$\left.\frac{\partial z}{\partial x}\right|_{i,j} = \frac{z_{i+1,j+1} - z_{i-1,j-1}}{2\sqrt{2}\Delta d} \tag{2.5a}$$

and

$$\left.\frac{\partial z}{\partial y}\right|_{i,j} = \frac{z_{i-1,j+1} - z_{i+1,j-1}}{2\sqrt{2}\Delta d}. \tag{2.5b}$$

Figure 2.4 shows an example of this method. By comparing the examples for the FCN and FDN algorithms (Figures 2.3 and 2.4), it can be seen that the values for slope
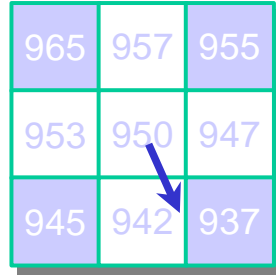
Figure 2.4: Example of the FDN method.

and aspect are slightly different for the two methods. Therefore, for this example at least, there is a slight grid bias.

2.3.3 Eight Neighbours

Eight Neighbours Unweighted (ENU)

When more than four grid points are used, it is possible to define a topographic surface from which slope and aspect values can be determined. One such algorithm uses the eight neighbouring grid points to calculate the slope and aspect, representing a third order finite difference algorithm (Sharpnack and Akin, 1969; Papo and Gelbman, 1984). As will be discussed below, the slope and aspect values obtained using this method are the same as those for a least squares linear trend surface fitted to these eight neighbouring grid points. The local slope in x and y can be found applying the relationships,

$$\frac{\partial z}{\partial x}\bigg|_{i,j} = \frac{(z_{i-1,j+1} - z_{i-1,j-1}) + (z_{i,j+1} - z_{i,j-1}) + (z_{i+1,j+1} - z_{i+1,j-1})}{6\Delta d} \quad (2.6a)$$

and

$$\frac{\partial z}{\partial y}\bigg|_{i,j} = \frac{(z_{i+1,j-1} - z_{i-1,j-1}) + (z_{i+1,j} - z_{i-1,}) + (z_{i+1,j+1} - z_{i-1,j+1})}{6\Delta d}. \qquad (2.6b)$$

An example of this method is demonstrated in Figure 2.5.

$$slope = 0.357$$
$$aspect = 171°$$
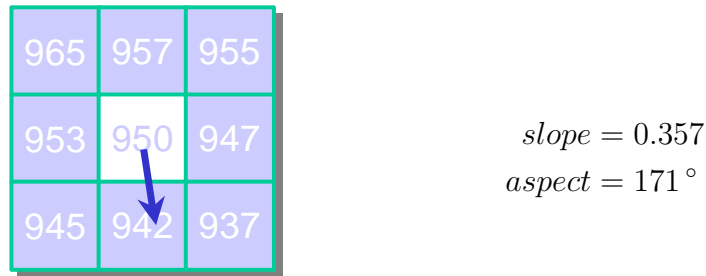
Figure 2.5: Example of the ENU method.

Multiple Linear Regression Models

If more than four elevation points are utilised in the determination of slope and aspect, either a terrain surface of a higher order then a plane can be modelled, or the additional points can be used to provide a least squares best fit solution (Guth, 1995). Examples of multiple linear regression models that can be used to model topographic surfaces, from which slope and aspect values can be determined, are provide by Evans (1980) and Zevenbergen and Thorne (1987). Their analysis of slope and aspect uses the eight neighbours in the DEM neighbourhood in relation to the central point. The two methods differ in whether or not the surface is forced to pass exactly through the grid points or whether a smoothing function is introduced. From the linearly regressed surface, slope and aspect can be found based on the calculations shown in Equations 2.1 and 2.2, given the values for the local slope in

x and y.

The linear regression model of Evans (1980) uses a full quadratic surface given by the equation

$$Z = Ax^2 + By^2 + Cxy + Dx + Ey + F, \tag{2.7}$$

where the nine elevations of the 3×3 submatrix are used to determine the six parameters, A through F, using least squares. This results in a surface that will not necessarily pass through the nine original elevations, hence introducing a slight smoothing of the surface. This smoothing is deemed acceptable since it helps to deal with minor data errors. Since the parameters are found using least squares, error can be incorporated into the estimate of slope and aspect. Solving for the local slope in x and y gives the following relationships,

$$\frac{\partial z}{\partial x} = 2Ax + Cy + D \tag{2.8a}$$

and

$$\frac{\partial z}{\partial y} = 2By + Cx + E. \tag{2.8b}$$

Zevenbergen and Thorne (1987) questioned whether the linear regression model presented by Evans (1980) could represent the land surface accurately since his model did not coincide with the nine elevations in the local neighbourhood. Therefore, Zevenbergen and Thorne (1987) used a modified surface which exactly passed

through the nine submatrix elements. The equation for such a surface is given by

$$Z = Ax^2y^2 + Bx^2y + Cxy^2 + Dx^2 + Ey^2 + Fxy + Gx + Hy + I, \qquad (2.9)$$

where the nine parameters can be determined from the nine elevations of the 3×3 submatrix by Lagrange polynomials. This leads to the equations for the slopes in x and y,

$$\frac{\partial z}{\partial x} = 2Axy^2 + 2Bxy + Cy^2 + 2Dx + Fy + G \qquad (2.10a)$$

and

$$\frac{\partial z}{\partial y} = 2Ax^2y + Bx^2 + 2Cxy + 2Ey + Fx + H. \qquad (2.10b)$$

It turns out that even though Zevenbergen and Thorne (1987) equation should produce a surface that fits better then Evans (1980), the two methods give identical values for slope and aspect of the central point (Skidmore, 1989; Guth, 1995). This is because slope is only estimated at a single point, which, through a suitable coordinate transform, can be given the coordinates (0,0). Each of the partial derivatives, therefore, only needs a single coefficient from the higher order surface, D and E for the six term quadratic polynomial and G and H for the nine term polynomial. This makes a calculation done by least squares, using either six or nine term polynomials, the same as a calculation done by applying a planar fit. It also turns out that the coefficients from which the slope and aspect values are calculated do not actually

depend on the central point for which the values are calculated. The results obtained by applying surface modelling are comparable to those found using the eight neighbours unweighted algorithm; however, the ENU algorithm is more computationally efficient (Hodgson, 1995).

Eight Neighbours Weighted

Numerical analysis suggests that an eight neighbour weighted algorithm will provide a better estimate for the local slopes in x and y (Horn, 1981). By giving the cardinal directions more weight then the diagonal directions, eight neighbour weighted algorithms lie between the four closest neighbour and eight neighbour unweighted algorithms. In this manner, the grid points that are closer to the central grid point are given a higher weight then the grid points farther away, hence they have a larger influence on the calculated slope and aspect values. While there are many possible weighting schemes, such as using one over the square of the distance (Jones, 1998), or one over distance squared (Horn, 1981), only one method, one over the square of the distance, is presented here. As with the methods discussed above, the only thing differentiating various weighting schemes is in how the local slopes in x and y are calculated, which is based on how much weight is given to the diagonal neighbours. The larger the inverse exponent is the less effect the diagonal neighbours have on the calculations at the central point. A squared inverse relationship with respect to distance was selected since most physical relationships exhibit such an association.

One Over Distance Squared (OODS) Horn (1981) implemented a slope and aspect algorithm in which grid point neighbours were weighted proportional to the reciprocal of the square of the distance from the central point. This generated

equations for local slopes in x and y given by

$$\left.\frac{\partial z}{\partial x}\right|_{i,j} = \frac{(z_{i-1,j+1} - z_{i-1,j-1}) + 2(z_{i,j+1} - z_{i,j-1}) + (z_{i+1,j+1} - z_{i+1,j-1})}{8\Delta d} \quad (2.11\text{a})$$

and

$$\left.\frac{\partial z}{\partial y}\right|_{i,j} = \frac{(z_{i+1,j-1} - z_{i-1,j-1}) + 2(z_{i+1,j} - z_{i-1,}) + (z_{i+1,j+1} - z_{i-1,j+1})}{8\Delta d}. \quad (2.11\text{b})$$

The slope and aspect for the central point is solved by applying the above equations to Equations 2.1 and 2.2 respectively. An example for this method is shown in Figure 2.6. The differences between the results presented in Figures 2.5 and 2.6, which

$$slope = 0.347$$
$$aspect = 168\,^{\circ}$$
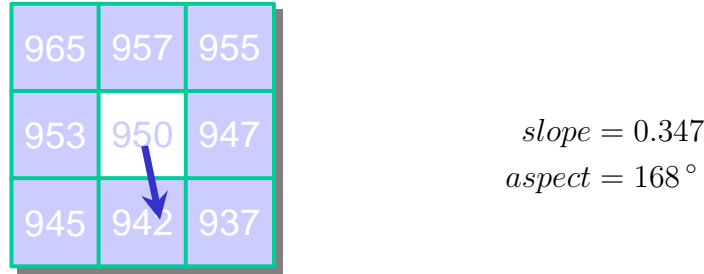
Figure 2.6: Example of the OODS method.

demonstrate the ENU and OODS algorithms respectively, indicate that in this example, the diagonal elements significantly influence the results of the ENU algorithm.

2.3.4   Steepest Neighbour

Hydrologically, DEMs are useful in the extraction of drainage networks. When looking at topographic parameters from a hydrological standpoint, it is not necessarily important how accurate the individual parameters are, but how accurate derived

characteristics such as drainage networks can be resolved. It is for this reason that steepest neighbour algorithms have been developed. These algorithms are more suited to finding parameters such as upslope area, discussed in Section 2.4.1, than finding accurate slope and aspect values, since they are more concerned with tracking flow paths. The basic concept behind steepest neighbour algorithms is finding the neighbour, out of the eight, which either has the smallest elevation value, or has the largest difference, when compared to the central point. It has been said that steepest neighbour algorithms are the only algorithms that actually use the elevation of the central points and all eight of its nearest neighbours (Guth, 1995). However, this statement might be a little misleading since though all eight neighbours are considered, only one is used to calculate the slope and aspect.

Maximum Downhill Gradient (MDG)

A model introduced by O'Callaghan and Mark (1984), finds the steepest downhill neighbour in order to determine topographic parameters such as slope, aspect, upslope area and drainage networks (Band, 1986; Jenson and Dominque, 1988; Fairfield and Leymarie, 1991). This method is based on an eight neighbour connectivity where the drainage direction (aspect) of the central point is taken as the direction to the neighbour with the maximum drop, i.e. the neighbour which is lower then the central point and is the minimum value. Problems arise when more than one neighbour fits the criteria simultaneously. There are, of course, different ways to deal with this problem, some of the more popular include arbitrarily choosing the first neighbour encountered when going through the neighbours clockwise from north, or flagging the point for later inspection. As mentioned in Section 2.1, problems are

encountered when the central point is a pit and no such minimum neighbour can be found. Specific implementations of this algorithm vary in terms of how they handle this special case. In this study, the first instance of the lowest neighbour was selected when going through the neighbours clockwise from north.

The slope value for the central point using the steepest downhill neighbour algorithm is calculated as the elevation difference between the neighbour with the minimum elevation and the central point,

$$slope = \frac{Z_{minNeighbor} - Z_{central}}{\Delta d}. \tag{2.12}$$

In order to compensate for the increased path length to diagonal neighbours (NE, SE, SW, NW), the slope values for the diagonal neighbours are adjusted by a factor of $1/\sqrt{2}$,

$$slope_{diagonal} = \frac{Z_{minNeighbor} - Z_{central}}{\sqrt{2}\Delta d}. \tag{2.13}$$

In this method it is assumed that the contour length is equal to the grid interval.

The aspect for the central point is defined as the direction to the neighbour with the minimum elevation. Based on the 8 neighbours defined in Figure 2.1, the aspect for a given point can only be represented by one of the eight main compass directions separated by 45° (N, E, S, W, NE, SE, SW, NW). Figure 2.7 illustrates an example of this method.

965	957	955
953	950	947
945	942	937

$$slope = 0.368$$
$$aspect = 135\,^{\circ}$$
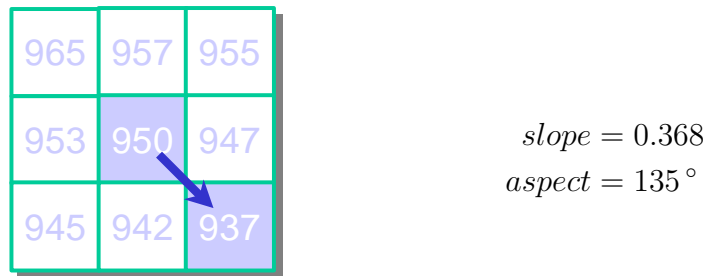
Figure 2.7: Example of the MDG method.

Multiple Downhill Neighbours (MDN)

One of the main drawback of the steepest downhill neighbour algorithm is that it is greatly effected by grid orientation bias. Truly accurate values for slope and aspect are not obtained because of the need to follow the major points on the compass. Multiple downhill neighbours methods (Quinn et al., 1991; Freeman, 1991; Quinn et al., 1991; Wolock and McCable Jr., 1995) are a variation of the steepest downhill neighbour algorithm which attempt to solve the limitations present when dealing with a one dimensional representation of flow. This is accomplished by distributing flow from a pixel among all of its lower elevation neighbour pixels. Slope and aspect are calculated by taking the average of the all the downslope neighbours, i.e. the average slope and aspect values. A numerical and pictorial example of this method is shown in Figure 2.8. Slope and aspect in this example are found by averaging

965	957	955
953	950	947
945	942	937

$$slope = 0.237$$
$$aspect = 158\,^{\circ}$$
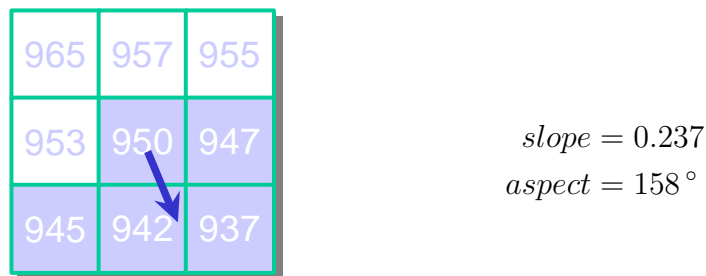
Figure 2.8: Example of the MDN method.

the slope and aspect values of all the downslope neighbours, which are highlighted in light blue. Slope and aspect for each individual downslope neighbour is found by applying the method outlined for the MDG(Equations 2.12 and 2.13).

Maximum Adjacent Gradient (MAG)

Another variation on the maximum downhill gradient algorithm is the maximum adjacent gradient algorithm (Skidmore, 1989; Guth, 1995). In this algorithm, the steepest slope is found among the eight neighbours, compensating for the distance to the neighbour cell, and assigned to the slope value. If the slope is uphill, the downhill aspect is considered to be in the directly opposite direction. This algorithm uses the same equations applied in the MDG algorithm, and hence suffers from the same limitations. Figure 2.9 illustrates and example of this method. In the example

$$slope = 0.424$$
$$aspect = 135\,°$$
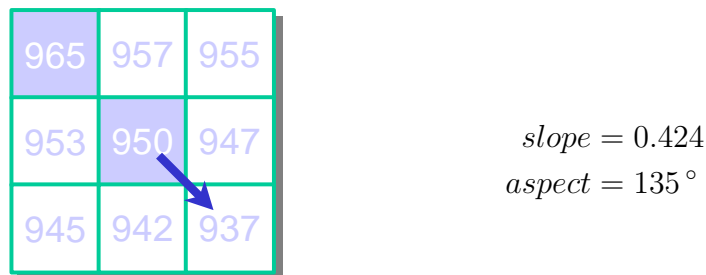
Figure 2.9: Example of the MAG method.

presented, the results of the MDG and MAG methods are the same, even though they are calculated using different neighbours. A result like this is dependent on the shape of the terrain and will not always be the case.

2.3.5   Comparison of Slope and Aspect Algorithms

Different slope and aspect algorithms will, of course, result in different slope and aspect values. Guth (1995), found that the choice of algorithm can vary the average slope by as much as 25%. Such a large variation emphasises the care that should be taken in selecting an algorithm that will produce an accurate representation of the terrain. The criteria for correctness needs to be based on the desired application. Solving for basic drainage networks could effectively be done using the steepest neighbour algorithms, but if something closer to the actual aspect value is required then the eight neighbours unweighted algorithm might be more applicable, since it provides results which more closely represent the terrain.

Comparing the "correctness" of slope and aspect algorithms can be done in a variety of ways. One method is to compare results for a surface with known slope and aspect values (Hodgson, 1995; Jones, 1998). The only way that known slope and aspect maps can be generated is if the terrain surface used for comparison is synthetic, i.e. it has been generated by a large term polynomial surface. Given the equation for the surface, actual values for the slope and aspect can be determined. Another method of comparison is to choose a method of determining slope and aspect that is considered to produce the "true" value, such as hand derived values from contour maps (Skidmore, 1989). If no truth values are available, the last alternative is to do statistical comparisons of the results obtained by the differing algorithms (Guth, 1995). However, a statistical comparison between methods really only investigates the variation between methods and cannot be used to compare estimates to ground measurements.

Based on the various comparisons done on slope and aspect algorithms (Guth,

1995; Skidmore, 1989; Hodgson, 1995; Jones, 1998), a few generalisations on the algorithms can be made. Surprisingly, algorithms utilising only four neighbouring cell values tend to be better at estimating slope and aspect values than algorithms using eight neighbouring cell values. Algorithms that use only one to two of the neighbouring cell values along with the centre value do not, in general, perform well. These two to three point algorithms normally perform significantly worse than the four closest neighbour algorithm, and should not be used when accurate slope and aspect values are desired.

2.4   Upslope Area

Upslope area is an important parameter in determining hydrologically significant terrain characteristics such as drainage networks. It represents not only the flow direction of water, but the accumulated area draining through a point. As mentioned previously, the calculation of upslope area is dependent on the determination of aspect. However, slope and aspect values can be determined using localised neighbourhood operations, upslope area calculations are fundamentally dependent on the entire DEM. Fortunately, they can be determined through the use of modified neighbourhood operations where values are passed down cell by cell.

For a gridded DEM, the upslope area can be generalised as the number of cells that drain into a specified cell multiplied by the area of a grid cell. For a given grid cell, the upslope area can be expressed as,

$$upslope\ area = N * \Delta d^2, \tag{2.14}$$

where N is the number of upslope cells and Δd is the grid spacing. Based on this relationship, a ridge point, i.e. a point that has no drainage inputs, would have a nonexistent upslope area, while a pit could have a very high upslope area since it can be drained into from all sides.

The determination of upslope area for each cell in a DEM can be difficult since it involves tracing flow paths through the entire DEM. While there are different ways this problem can be solved, one of the computationally simplest in terms of programmability is through the use of a recursive algorithm (Tarboton, 1997; Freeman, 1991). The first step in this process is, of course, to determine the two dimensional flow direction of each cell in the DEM. Besides the aspect grid, two other grids are required, an inflow count grid and an upslope count grid. The cells in the inflow count grid contain a count of the number of cells that flow into them, while the cells in the upslope count grid contain a count of the number of upslope cells. To determine the inflow count grid, each cell is initialised to zero. Then, using the aspect grid, the values of the cells in the inflow count grid are incremented for every cell that drains into them, in other words, every time the flow is directed towards the cell. In this way, the values of the inflow count grid can range from zero to eight (none to all of the neighbours). For the upslope count grid, the cells are initialised to one. The inflow count grid is then gone through until a zero value is found. This indicates that a cell that has no upslope neighbours. The count of the upslope count grid cell (or cells) that the zero valued cell flows into is then increased by adding the zero cell's upslope area (or portion of). This flow direction is determined using the grid of aspect values. The inflow grid cells involved, including the zero valued cell, all have their values decreased by one. This process is repeated, adding cell outflows

iteratively to lower neighbours, until all the cells in the inflow count grid are negative. The values in the upslope count grid indicate how many cells are upslope of a given cell. The upslope area for each cell is found by multiplying by the area of each grid cell (Equation 2.14).

While the procedure outlined above is the general method used to determine upslope area, the calculation of upslope area, like the calculation of slope and aspect, can be determined in different ways. The main difference between these methods is how they deal with flow divisions, i.e., flow can either be restricted to exactly one downslope neighbour, or divided according to either the number of downslope neighbours or the aspect direction. The choice of how to divide flow is based on how the flow direction (aspect) is determined. Any of the methods described in Section 2.3 can be used to determine the flow direction of a cell, though some algorithms are more suited to specific upslope area algorithms then others. Algorithms used to determine upslope area are presented in the following sections along with the aspect algorithms they best compliment. Also included are some of the algorithms' strengths and weakness.

2.4.1   Single Flow - Steepest Downhill Neighbour

The steepest downhill neighbour upslope area algorithm (O'Callaghan and Mark, 1984) goes hand in hand with the MDG algorithm for determining slope and aspect, although it can be used with the MAG algorithm (Band, 1986; Jenson and Dominque, 1988; Fairfield and Leymarie, 1991). In this method flow can only be routed to one downslope neighbour. The flow direction, as with the MDG and MAG algorithms, is restricted to one of the cardinal or diagonal directions. This allows flow to be traced

with very little dispersion, hence making the determination of drainage networks easier. Because of the simplicity of this method and the lack of dispersion, this is generally the choice of upslope algorithms from a hydrological standpoint.

Despite the popularity of the steepest downhill neighbour upslope area algorithm, many authors have drawn attention to its drawbacks (O'Callaghan and Mark, 1984; Band, 1986; Fairfield and Leymarie, 1991; Costa-Cabral and Burges, 1994; Skidmore, 1989; Guth, 1995; Tarboton, 1997; Wolock and McCable Jr., 1995). The main problem with this method is that it suffers from grid orientation bias. This can dramatically throw a drainage path off course by as much as 44°. In the extraction of drainage networks, this discretization can prevent stream formation due to the generation of parallel flow lines especially in relatively flat areas. The rougher the terrain, however, the less significant this problem is. The limitations of this method have prompted the development of other algorithms.

2.4.2   Stochastic Method

Fairfield and Leymarie (1991) applied a stochastic version of steepest downhill neighbour upslope area algorithm in which the drainage direction was chosen probabilistically. Using their algorithm, flow direction is randomly assigned to one of the downslope neighbours, with the probability proportional to slope. In this method the greatest downhill slope is not always taken in order to more faithfully follow the true aspect of the land. This algorithm attempts to alleviate some of the problems of grid bias, where the flow path must follow one of the cardinal or diagonal direction resulting arbitrarily from grid orientation. While this method does provide more appropriate flow path directions, it introduces problems of its own (Costa-Cabral and

Burges, 1994). Randomness does not ensure reproducible results, making it difficult to get comparable values. There are also problems in flat areas where flow should be parallel. In the stochastic method adjacent flow paths are not parallel but "wiggle" randomly often converging laterally with one another. Once converged, flow paths are nearly impossible to separate, hence flow becomes more and more concentrated downslope.

2.4.3   Multiple Flow - Steepest Downhill Neighbours

The multiple downhill neighbours algorithm for slope and aspect (Section 2.3.4) is utilised in multiple flow upslope area algorithms. In this method, flow directions are still resticted to the cardinal or diagonal grid cells, but unlike the single flow method, flow is partitioned to all the downslope neighbours. The amount of flow partitioned to each downslope neighbour is based on the size of the slope. The larger the slope the more of the flow that is partitioned to it. For a grid cell with an upslope area of A and n downslope neighbours, the upslope area partitioned (Ap) to each downslope cell i is given by,

$$Ap_i = A * \frac{slope_i}{\sum_1^n slope_i}. \tag{2.15}$$

From a drainage network perspective, the multiple flow upslope area algorithm can significantly disperse the water flow depending on the type of terrain, which can be problematic (Skidmore, 1989). The multiple direction method tends to perform poorer in flat areas then the single direction approach, but can produce more realistic flow palths in steeper terrain (Quinn et al., 1991). While it is possible to more

accurately resolve the flow path in a DEM using a multiple flow direction algorithm, the significant dispersion introduced does not make this method a popular choice in some terrain.

2.4.4   Plane Fitting

Plane fitting uses the aspect associated with each pixel to specify flow direction (Tarboton, 1997), and is conducive to any of the slope and aspect algorithms in which the aspect does not necessarily point directly to one of the eight neighbours (including TPP, FCN, FDN, ENU and OODS). Flow is routed as though it were a ball rolling on a plane released from the centre of each grid cell. Flow in this algorithm is not restricted to the cardinal or diagonal directions. Therefore, this method has the advantage of being able to, in a sense, specify flow continuously. If the aspect angle does not lie directly on one of the cardinal or diagonal directions, flow is partitioned, based on the angle, between two cells. Problems encountered with this method are normally related to discontinuous representations of the surface at pixel edges that lead to inconsistent or counter-intuitive flow.

Chapter 3

The Topographic Index and TOPMODEL

Gridded DEMs usually cover rectangular regions. However, what is of interest hydrologically is not generally a rectangular piece of terrain but a watershed or catchment area. Watersheds are geographical regions that do not receive inflow from outside the region itself. Outflow from a watershed can be channeled through one or many outlets, but what is investigated here are watersheds with a single outlet. Because the surface flow in a watershed is self-contained, it is possible to model the hydrological interactions.

The hydrological model used in this research is called TOPMODEL (*top*opgraphic *model*). TOPMODEL attempts to model, among other things, the discharge rate (Q) from a watershed's outlet as a result of rain events. An important parameter used by TOPMODEL is the topographic index.

3.1 The Topographic Index

The topographic index is used to represent the soil saturation (Beven and Kirkby, 1979; Wolock and McCable Jr., 1995; Quinn et al., 1995). It is an estimate of the accumulated water flow at any point in a watershed. A high topographic index indicates that the ground in a region has a higher potential to be saturated, while a low topographic index indicates the ground is less likely to be saturated. Areas of saturation are the source areas for overland flow. Generally, high values of the topographic index occur in flat areas with little slope and/or in regions with a large upslope area.

In Chapter 1, it was stated that the topographic index is equivalent to the natural log of upslope area divided by the slope ($\ln(A/slope)$). This is, however, somewhat of an oversimplification. More specifically, it is the natural log of the *specific* catchment area (a) divided by the slope,

$$topographic\ index = \ln\left(\frac{a}{\tan\beta}\right).\tag{3.1}$$

By convention, in the equation for the topographic index the slope is represented by $\tan\beta$, where β is the slope angle. The slope is used to approximate, under steady state conditions, the local hydraulic gradient – i.e. the slope to the water table.

The specific catchment area is defined as the upslope area per contour length. Expressly, it is given by

$$a = \frac{A}{l},\tag{3.2}$$

where l is the contour length, and, as before, A is the upslope area. Another way of describing the specific catchment area is to say that it is the area above a certain contour length that contributes flow across the contour (Gallant and Wilson, 2000). Figure 3.1 illustrates such an area. For gridded data, the contour length can be given a value equivalent to the grid spacing.
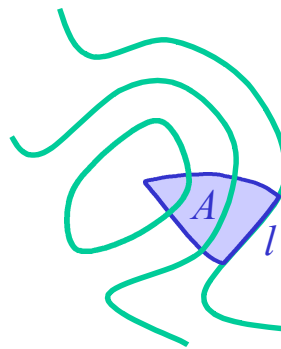
Figure 3.1: Specific area (a): the upslope area per contour length ($a = A/l$).

The topographic index is calculated for each cell in a DEM. To do this, the slope, aspect and upslope area must first be calculated using, for example, one of the algorithms discussed in Chapter 2. The $\tan\beta$ term is equivalent to the slope in the aforementioned algorithms.

While the topographic index is calculated for each cell, it is computationally easier to deal with a discretised distribution function, where the number of cells with a given topographic index is plotted as a function of the topographic index. An example of such a distribution function is shown in Figure 3.2. As will be discussed in Section 3.2, a main assumption in the hydrological model used in this research is that cells with the same topographic index are hydrologically similar, and that the spatial distribution of the topographic index can be used to approximate the

spatial distribution of the water table depth. Therefore, the generation of a spatially distributed water table does not require calculations for each individual cell, but rather a single calculation for each topographic index class.
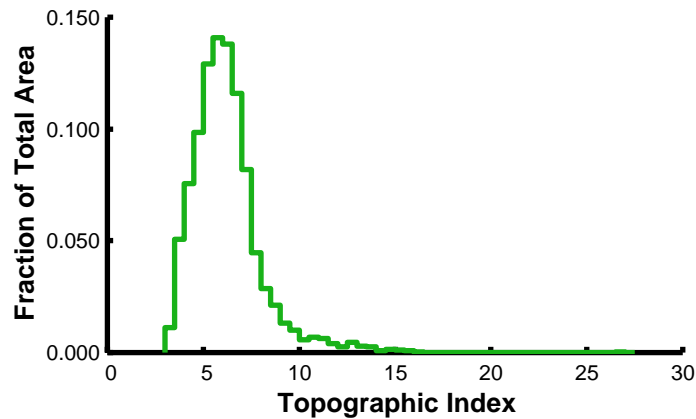
Figure 3.2: Topographic index distribution function. Values are binned at 0.5 intervals.

3.2   An Introduction to Topmodel

TOPMODEL is a distributed, or more specifically a semi-distributed, hydrological model (Beven and Kirkby, 1979). A hydrological model attempts to predict the flow of water across terrain in response to rain events. The output from these models is summarised by a hydrograph, which is the discharge rate of flow at the watershed's outlet. The hydrographs generated by TOPMODEL include both the surface runoff and the subsurface flow. A hydrological model is said to be distributed when it takes into account the patterns of hydrological variables in a watershed, instead of using single values for the entire area. TOPMODEL can be considered semi-distributed

since it uses lumped or binned values of the topographic index to characterise the saturated areas of a watershed, as opposed to values at every location on the surface.

TOPMODEL is based on a simplified physical model. This keeps the number of input parameters to a minimum. Three primary assumptions are used in the simplification. These are (Beven and Kirkby, 1979):

- The dynamics of the saturated zones can be approximated by successive steady state representations

- The local hydraulic gradient of the saturated zones can be approximated by the local ground slope ($\tan \beta$) (Darcy's Law)

- The distribution of downslope transmissivity with depth may be described by an exponential function of storage deficit

These assumptions lead to the topographic index being used as the index of hydrological similarity, as stated in the previous section.

The topographic index alone is not enough to characterise the hydrological behaviour of a watershed. Therefore, in addition to the topographic index, TOPMODEL uses a number of other parameters that are uniquely determined for the entire watershed. As mentioned in the assumptions, the downslope transmissivity of the terrain is required in order to determine subsurface flow. Thus, one parameter used by TOPMODEL is the downslope transmissivity at soil saturation (T_o). One of the more important parameters in TOPMODEL is the saturated zone, or recession parameter m. This parameter is the coefficient of the exponential decrease of hydraulic conductivity with depth. Two other parameters used by the model are the initial and maximum storage deficits in the root zone, indicated by SR_o and SR_{max}, re-

spectively. Another parameter is the overland flow speed (RV), which is used for internal routing. Depending on how TOPMODEL is used, there may also be other parameters required than those described above. However, in this research only this set of parameters was used. While the parameters for TOPMODEL can be determined through field measurements, they are generally optimised through model calibration as is discussed in Section 3.3.

In addition to watershed-specific parameters, TOPMODEL also requires input data for the rain event that is being studied. TOPMODEL is run for a given watershed, over a specific time series, at a set time step (Δt). Therefore, for each time step, TOPMODEL requires the precipitation ($R(t)$) and the potential evapotranspiration ($PE(t)$). Additionally, the initial flow rate (Q_o) of the outflow and channel routing variables are needed. Channel routing describes how much of the cumulative area of the catchment (ACH) is routed through a specific length of the mainstream (D). To calculate how well the model predicted hydrograph represents reality, field values of the discharge per time step are required ($Q(t)$). Given these values, TOPMODEL can calculate statistics on how well the predicted hydrograph matches reality. These statistics include an efficiency value (EE) and the rms difference.

The role of the topographic index in TOPMODEL is to determine the zones of saturation. The local saturated zone deficit S for each topographic index class i is calculated for each time step as

$$S_i = \bar{S} - m \left[\lambda - \ln \left(\frac{a}{\tan \beta_i} \right) \right], \tag{3.3}$$

where λ is the mean topographic index, and $\bar{S}$ is the mean storage deficit. This equation is used to determine the parts of the watershed that have no storage deficit

and are in a saturated state ($S_i \leq 0$). Saturated areas are the regions that contribute to overland flow, generating the predicted discharge flow rate.

In this research, TOPMODEL is implemented in a basic form. Only a brief description of TOPMODEL and how it uses the topographic index has been presented. More detailed descriptions of the model, along with applications, can be found in a variety of sources, including Beven and Kirkby (1979); Bruneau et al. (1995); Quinn et al. (1995); Wolock and McCable Jr. (1995) and Franchini et al. (1996).

3.3 Calibration of Topmodel

Models, such as TOPMODEL are simplifications of physical processes. However, in the natural environment, it is impossible to know or model all variables, and because of this, models cannot reproduce the behaviour of a natural environment in all its detail. Therefore, it is normally necessary to optimise model parameters in order to obtain realistic results. Optimisation of a model's parameters is termed the calibration process – i.e. the model is calibrated to produce optimal (or, at the very least, reasonable) output. In TOPMODEL's calibration process, the parameters themselves may be assigned values outside their physically realistic range, but this is done to compensate for model deficiencies. Traditionally, models are calibrated for one time series, and the calibrated parameters are then used to run the model for other events in the same watershed. Optimisation can be done either by hand or with use of an automated optimisation scheme. The starting point for calibration of the parameters is generally an estimate of field values.

3.4 Implications of the Shape of the Topographic Index Distribution Function

The main objective of this research is to investigate the effect of errors in DEMs on applications that use them. The only parameter used by TOPMODEL that has any relation to a DEM is the topographic index distribution. Therefore, presented here are some of the characteristics of topographic index distributions and their possible impact on TOPMODEL results.

The topographic index distribution function can be described by its mean, standard deviation and skewness. From Equation 3.3, it is apparent that the mean topographic index plays an important role in determining saturated area, and as a consequence the amount of overland flow. In Wolock and McCable Jr. (1995), it was shown that an increase in the mean causes a decrease in the amount of subsurface flow, and as a consequence, an increase in the amount of overland flow. The decrease in the subsurface flow, in turn, decreases the average depth to the water table, which increases the possibility that saturated areas will develop, thus producing overland flow. An increase in the standard deviation of the topographic index tends to increase the size of saturated areas, since it is an indication of the width of the distribution and the amount of area that will become saturated. The skewness gives an indication of the lopsidedness of the distribution curve. Since the size of the saturated area is determined primarily by the area of the topographic distribution that is greater than the mean, a large skewness in values greater then the mean can have an impact on certain conditions. For example, under dry conditions, the more skewed the distribution, the larger the possibility of saturation and hence, the

greater the amount of overland flow. This corresponds to an increase in the peak discharge values. In contrast, under highly saturated conditions, the skewness might not have a significant impact on the predicted hydrograph, since more of the area will be saturated anyway.

The shape of the topographic index distribution function affects the runoff dynamics of TOPMODEL (Quinn et al., 1995). However, it is possible, through calibration and re-optimisations of the calibrated parameters (described in Section 3.3), to compensate for a poor distribution. This means that a parameter set can be optimised using almost any topographic index distribution to produce an adequate hydrograph, but at the cost of calibration parameters that are unrealistic even by the fairly accommodating standards of TOPMODEL. It therefore stands to reason that if a comparison of topographic distributions for a watershed is desired than the model should be calibrated once, and the resulting hydrographs from the different distributions compared.

Chapter 4

Study Area and Data Set

4.1 Terrain Data

The DEM used in this study was taken from a series of gridded DEMs provided by the province of Alberta, Canada. These DEMs have extents that coincide with provincial 1:20000 scale map sheets. Depending on the roughness of the terrain, the DEMs were originally collected from aerial photographs at spacings of 25 m, 50 m, or 100 m. They were then interpolated to 25 m grids by linear least squares prediction using the SCOP program (Ackermann, 1992). For the northing and easting co-ordinates, the resulting DEMs have a specified rms accuracy of ± 10 m 90% of the time. The elevations have a specified rms accuracy of ± 3 m 90% of the time. The remaining 10% not within this bound has a specified accuracy of ± 5 m 90% of the time. For this study, the error in planimetry was ignored, while the rms error in the elevation was taken to be 3 m.

From the available DEMs a watershed was extracted that served as the study area.

The watershed selected, Marmot Creek main stem near Seebe, was drawn from the DEM that coincided with the provincial map sheet C82J14NE. The region covered by this map sheet is located in the Kananaskis region of Alberta, in the front ranges of the southern Canadian Rockies. The watershed, depicted in Figure 4.1, covers an area of approximately 10 km^2 (15484 grid cells). Elevations in the watershed DEM ranged between 1584.904 m and 2837.548 m. The stream outlet gauge, shown as a blue dot in Figure 4.1, is located at UTM coordinates (5645700 N, 629825 E) and is at an elevation of 1585 m. Extraction of the watershed from the DEM was performed using watershed selection tools available in the GIS software Arc/Info.
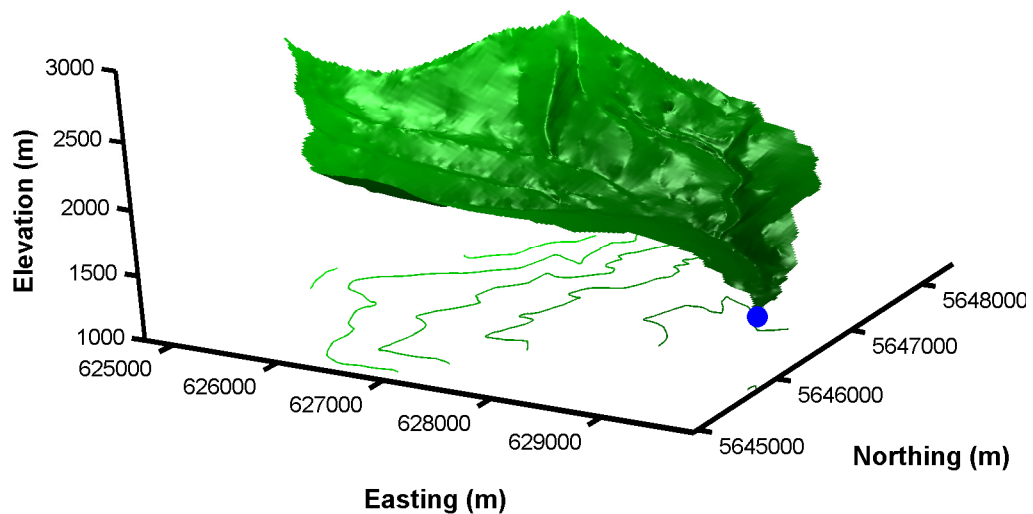
Figure 4.1: DEM of the Marmot Creek Main Stem watershed in Kananaskis, Alberta. The blue dot is the location of the stream outlet gauge.

4.2 Precipitation and Stream Discharge

The hydrological analysis of a watershed requires a time series of precipitation and stream discharge data for rain events. This data is used in TOPMODEL, for both model calibration and analysis. However, the assumptions used in TOPMODEL restrict the type of rain events that should be used. In particular, TOPMODEL does not take into account snow melt, and hence, rain events are restricted to periods and locations when and where this does not occur. In the Kananaskis region, snow can be found in some areas well into the summer, and it is only in August and early September that the region can be considered snow-free. Another consideration that must be made when selecting rain events for use in TOPMODEL is that the model was originally designed for areas that were both humid and temperate. Unfortunately, the Kananaskis is not normally humid. Consequently, the rain events for this area should be chosen during as wet a period as possible.

The above restrictions, combined with a limited availability of precipitation and rain gauge data, meant that the selection of rain events for the study area was limited. The rain events chosen occurred during a 200 hour time period that began at 01:00, August 1, and ended at 08:00 August 9, 2000. The total volume of rainfall for this time period was 30.9 mm and the total observed overland flow was 6.2 mm. There were two distinctive rain events during this period. These are visible in the hydrograph depicted in Figure 4.2. Characteristics of the hydrograph and the two rain events are provided in Table 4.1. The initial flow velocity of the stream at the beginning of the time series (Q_o) was $3.08{\times}10^{-5}$ m/h. The time to peak indicated in this table is the time between the rain event and the peak discharge.

Hourly precipitation data was provided by the University of Calgary's Kananaskis
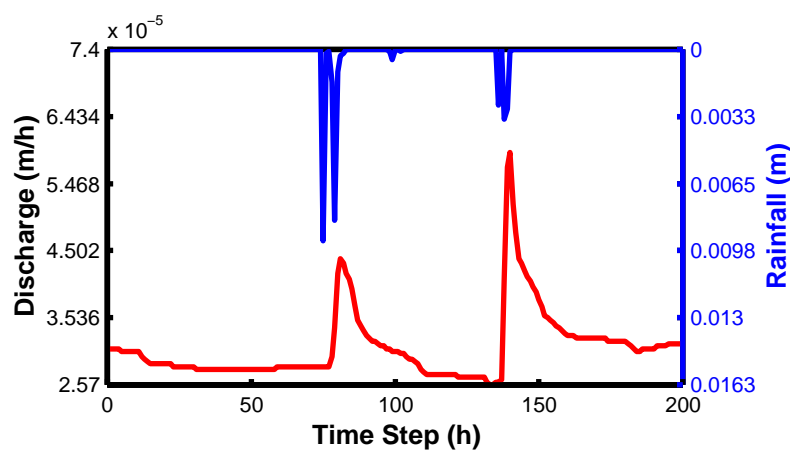
Figure 4.2: Hydrograph of the rain event. The 200 hour time series is from 01:00, August 1, to 08:00 August 9, 2000.

Table 4.1: Observed hydrograph characteristics.

Time to Peak (h)		Discharge of Peak (m/h)	
1	**2**	**1**	**2**
4.1	3.5	4.39×10^{-5}	4.76×10^{-5}

Field Station, while hourly stream discharge data was obtained from the Water Survey of Canada. Unfortunately, the precipitation data was not collected at the location of the stream discharge gauge but at the Kananaskis Field Station located at UTM coordinates (5654735 N, 637810 E) and an elevation of 1385 m. This means that the collection of the stream discharge data occurred approximately 8 km away and 200m higher than the precipitation data. In mountainous terrain, like the Kananaskis, the weather conditions can be dramatically different from one valley to the next and it is entirely possible that locations 8 km apart could experience different weather conditions. Possible differences between the provided precipitation data and the actual precipitation in the selected watershed can be seen in the hydrograph

(Figure 4.2), and in Table 4.1.

In addition to the hourly precipitation data, University of Calgary's Kananaskis Field Station also provided hourly temperature data, wind speed and the number of daily sunlight hours. This data was used to calculate the hourly potential evapotranspiration (PE) using the FAO Penamn-Monteith Method (Monteith, 1965).

4.3 Topmodel Calibration

Before TOPMODEL is used to predict discharge from a watershed it must first be calibrated. In such a calibration the goal is to match a hydrograph calculated by the model to an observed hydrograph. In this study calibration was done by trial-and-error, where the calibration parameters were manually adjusted until the resulting hydrograph had the best fit with the observed hydrograph. Described below are the input parameters used to calibrate TOPMODEL and the results of calibration.

4.3.1 Input Parameters

In order to calibrate TOPMODEL for a particular watershed, data specific to the watershed is required. Some of this data includes the hourly precipitation and discharge data (Figure 4.2), along with the hourly potential evapotranspiration. Also required by TOPMODEL is information on channel routing. Channel routing provides the model with information on how much area of the watershed is routed through a given length of the primary drainage route. For the purpose of channel routing in this study, the watershed was divided as evenly as possible into two sections. The accumulated area and distance to the drainage outlet were determined using Arc/Info,

and are shown in Table 4.2.

Table 4.2: Channel routing parameters.

Cumulative Catchment Area: ACH (%)	Distance from Outlet: D (m)
0.0	0.000
54.5	3411.701
100.0	5721.625

In addition to hydrological data, TOPMODEL also requires topographic data. The topographic data required by TOPMODEL is the topographic index distribution. Even though one of the objectives of this research is to compare different methods of calculating the topographic index, the model first has to be calibrated using only one of the methods. However, for later comparison of results, TOPMODEL was calibrated twice using two different topographic distributions, MDG and ENU. MDG is the method traditionally used in hydrology, so it is the natural choice for calibration. ENU, on the other hand, was selected because it was the method predicted to be the least sensitive to DEM error. The two topographic distributions used for calibration are shown in Figure 4.3. Topographic indices in these distributions were binned in intervals of 0.5. The two distributions have distinctive differences. The MDG topographic distribution has a slightly lower mean then the ENU distribution, but its skewness is larger (see Table 4.3). Because of the dry conditions of the watershed, the large skewness of the MDG distribution will likely be important in the height of the discharge peaks.
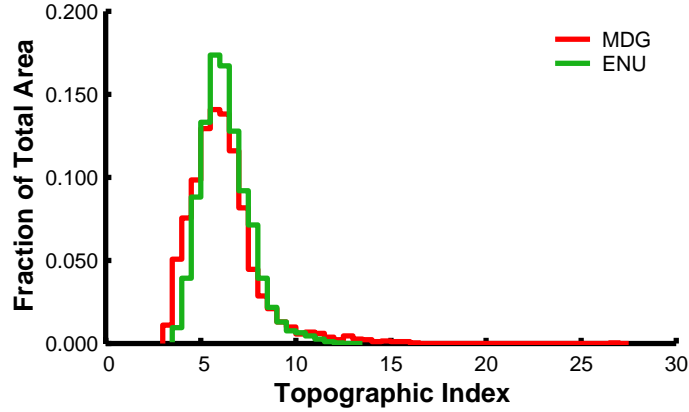
Figure 4.3: Calibration topographic distributions.

Table 4.3: Characteristics of the calibration topographic index distributions.

Characteristic	MDG Calibration	ENU Calibration
Mean	6.47	6.57
Standard Deviation	5.85	3.60
Skew	1.04	0.51

4.3.2 Calibration Parameters

In the calibration of TOPMODEL, four parameters – m, K_o, SR_{max} and RV – were adjusted. Not mentioned before is K_o, which is the hydraulic conductivity of the soil. It is used, along with m to determine T_o. Because the time series used occured after a dry period, SR_o was set equal to SR_{max}. The overland flow speed, RV, was set to a constant value of 3800 m/h, but a scaling parameter, $RFAC$, was introduced, and was the value calibrated. RV had to be scaled to compensate for the extended time delay between the rain events and the discharge responses. During calibration, these parameters were modified until the Nash-Sutcliffe Efficiency (EE) (Nash and

Sutcliffe, 1970) of resulting hydrographs was close to 1.00 as possible. The EE value was calculated as

$$EE = 1 - \frac{\sigma_E^2}{\sigma_Q^2}, \tag{4.1}$$

where σ_E^2 is the variance between the estimated and observed hydrographs, and σ_Q^2 is the variance in the observed hydrograph. The resulting calibrated hydrographs are depicted in Figure 4.3.2, with the numerical characteristics outlined in Table 4.4.

Table 4.4: Calibrated hydrograph characteristics.

Characteristic	Observed	MDG Calibration	ENU Calibration
Time to Peak 1 (h)	4.1	6.1	6.1
Time to Peak 2 (h)	3.5	4.5	4.5
Discharge of Peak 1 (m/h)	4.39×10^{-5}	4.71×10^{-5}	4.75×10^{-5}
Discharge of Peak 2 (m/h)	4.76×10^{-5}	5.48×10^{-5}	5.47×10^{-5}
Total Overland Flow (m/h)	n/a	4.07×10^{-3}	2.97×10^{-3}
Total Dishcharge (m/h)	n/a	6.22×10^{-3}	6.22×10^{-3}
RMS Error	n/a	3.05×10^{-6}	3.04×10^{-6}
Efficiency	n/a	0.636	0.640
Percent Difference Between Calibrated and Observed (%)			
Time to Peak 1		48.8	48.8
Time to Peak 2		28.6	28.6
Discharge of Peak 1		7.29	8.20
Discharge of Peak 2		15.1	14.9

Even with the best fit possible, the resulting calibrated hydrographs do not match the observed values very well. Since all that is of interest is an error sensitivity analysis, the fact that the model hydrographs do not match reality is ignored. The observed hydrograph is only used for calibration, and is not used further. Later

model comparisons will be made to the appropriate calibrated hydrograph.

While the difference between the two calibrated hydrographs are very small, the differences in the values of the calibrated parameters are more pronounced. These values are provided in Table 4.5, along with estimates of their true value. By examining the results in this table, it appears that the ENU method produces values that are closer to the estimated true values. This indicates that, for TOPMODEL at least, this method produces a topographic distribution that is more realistic for this watershed. However, both methods produce parameter values that are significantly different from those estimated, demonstrating that calibration is compensating for model deficiencies.

Table 4.5: Calibrated parameters.

Parameters	Estimated	MDG Calibration	ENU Calibration
m (m)	0.02688	0.03527	0.03519
K_o (m/h)	13.2	18.7555	7.1000
SR_o (m)	0.06	0.0190	0.0189
SR_{MAX} (m)	0.04	0.0190	0.0189
RV (m/h)	n/a	3800	3800
$RFAC$	n/a	0.27	0.27
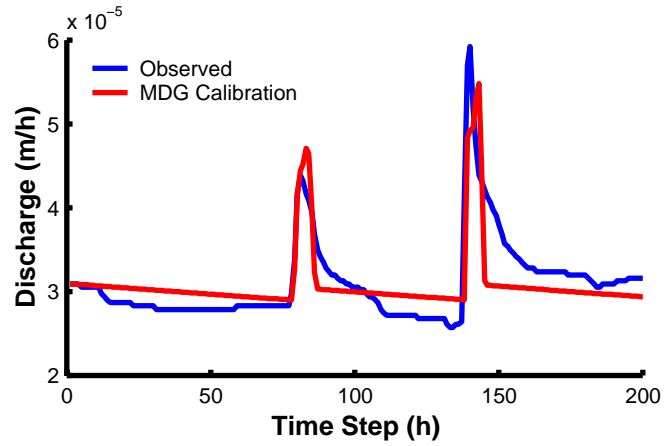
(a) MDG
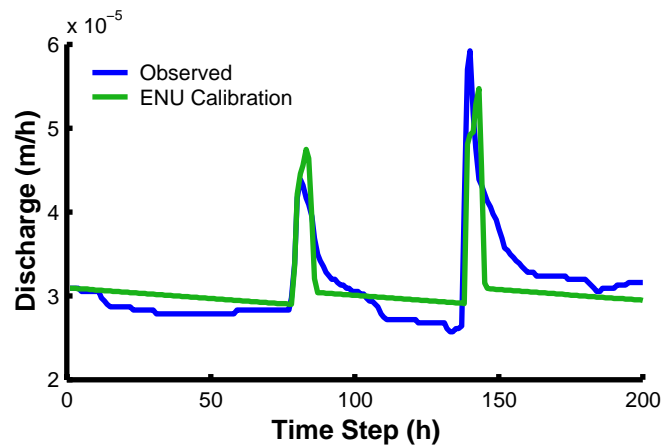
(b) ENU

Figure 4.4: Calibration hydrographs.

Chapter 5

Experimental Methodology and Implementation

5.1 Propagation of Error

DEMs have errors in both planimetry and elevation. In the algorithms for slope and aspect – the values upon which other topographic parameters are based – only the grid spacing and elevation values are required. This means that as long as the grid spacing is constant, any other errors in planimetry can safely be ignored. For any DEM that has been collected on a regular grid, or interpolated to one, the grid spacing is virtually guaranteed to be constant. Errors in planimetry may still exist; however, they would probably be in the form of a translation error, where the entire grid has been shifted from its true location. There may also be a scale error, where the grid interval is slightly smaller or less-than the specified interval, but this difference is most likely insignificant and could be disregarded. In any case, errors in planimetry

will manifest themselves as errors in elevation. Thus error analysis on parameters derived from gridded DEMs can be based purely on elevation error.

There are a variety of methods that can be used to propagate error. These methods include an analytical approach, Taylor series expansions, and Monte Carlo simulation (Heuvelink, 1998). In the analytical approach, the mean and standard deviation of a function is explicitly derived. This is dependent on knowing the exact form of the function involved. In methods based on Taylor series expansions the function is approximated by a truncated Taylor series from which the mean and standard deviation are determined. Neither of these methods of error propagation are suitable to the error analysis of this study. While it is possible to use these methods to determine the error in some of the topographic parameters, they cannot be used for all those investigated. Problems arise with the slope and aspect algorithms that are based on the steepest neighbour principle (MDG, MAG and MDN). These algorithms are decision-based, involving the selection of neighbours based on specific properties. Such algorithms do not have the functional form required by the analytical and Taylor series approaches. Another limitation of these approaches is that they are restricted to neighbourhood operations. They are not suitable for global operations, such as the calculation of upslope area, and, by extension, the calculation of the topographic index (Heuvelink, 1998). Also, because of complex model structure and dynamics, these error propagation methods are difficult to implement for a hydrological model. Therefore, the effect of error in a DEM on its derived parameters and on hydrological modelling is best determined with statistical analysis using Monte Carlo simulation and error realisations of the DEM (Veregin, 1997).

5.1.1 Monte Carlo Method

In the Monte Carlo method of error analysis, a given algorithm is repeatedly applied to sets of random input data. Each set of random input data is termed a realisation, and all the realisations are generated from the same error distribution. The realisations represent possible error-free data sets, and not just a data set with an added error component. Using the results from all the realisations, it is possible to calculate a mean and standard deviation that correspond to the algorithm under analysis. The mean is considered the 'actual' value that the algorithm would produce, while the standard deviation is considered the error. Because the analysis of results from a Monte Carlo simulation is done using statistical – and not analytical – quantities, the method is said to use a stochastic approach to error propagation (Heuvelink, 1998).

A simple Monte Carlo simulation of DEM error simulates values for each grid cell independent of the rest of the surface. The error simulation process begins with the generation of random error grids that have the same dimensions as the original DEM. The values in the error grids are generated from a normal probability distribution that has a standard deviation (stdv) equal to the rms error of original DEMand a mean of zero. The error grids are then added to the original DEM, creating a realisation of the original DEM.

The Monte Carlo method of error propagation is advantageous for this study because it is not affected by the exact formulation of the algorithms. Instead, it simply treats the algorithms as 'black boxes' whose response to the error in input is studied from the resulting outputs. Therefore, with Monte Carlo simulation it is possible to determine the actual effect of error, regardless of global operations or a

selection process in the algorithms.

The primary disadvantage of the Monte Carlo method is the computational requirements. In order to produce statistically reliable results, a large number of realisations should be run. Obviously, a difficulty with the approach is determining exactly how many times an algorithm should be implemented in order to minimise the computational load, while still insuring reliable results. A few studies have been done where only a few runs have been used (20-50) (Fisher, 1991a; Holmes et al., 2000), but other research has shown that this is not enough to produce reliable results (Veregin, 1997).

5.1.2   Generation of Error realisations

In the literature, choosing the number of realisations that are used in Monte Carlo error simulations often seems to be fairly arbitrary. In order to avoid a similarly arbitrary selection in this research, a more substantial method was required. The method used was based on the simple idea that realisations are only required if they significantly effect results. For example, if using 500 realisations produces the same result as using 200 realisations, then there is no need to us the additional 300 realisations. To apply this method, it is first necessary to generate realisations using the same error distribution. As the number of error realisations is increased, the standard deviation of each grid cell over all the realisations is determined, and a grid of standard deviations is generated. The standard deviation of this grid of standard deviations is found after the addition of each realisation, and this value is compared with the previous value. If the change in the standard deviation is not significant, then the addition of the realisation does not introduce any new

information. Therefore, any realisations after this point would be redundant.

An example of this procedure is shown below in Figure 5.1. In this figure, the standard deviations versus the number of realisations are plotted for error realisations generated using a standard deviation of 3 m. After 500 realisations the curve begins to level out, and adding additional realisations has little impact on the resulting standard deviation. Consequently, a Monte Carlo simulation using 500 realisations would be enough to produce statistically reliable results.
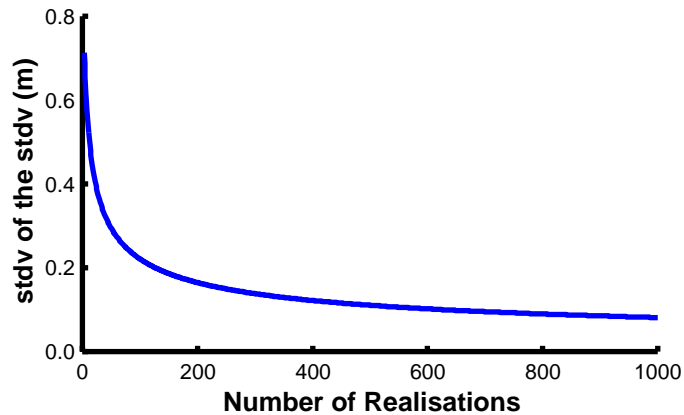
Figure 5.1: The standard deviation of the standard deviation error matrix for uncorrelated random error with a standard deviation of 3 m. The standard deviation of each grid cell is taken over the number of realisations specified. The standard deviation is then taken of the standard deviation matrix.

It should be noted that as long as the standard deviations of the error realisations are the same, the size of the grid used does not matter since the resulting shape of the curve does not change. The only change that can be seen is a slight vertical displacement, where the smaller the grid the higher the standard deviations.

5.1.3 Correlated Error

Up to this point it has been assumed that DEM error is uncorrelated in nature. However, this is, in effect, a worst case scenario, as in reality the error in DEMs tend to be positivity correlated with distance. In other words, the closer points are to each other, the more related their errors are. This has much to do with the terrain characteristics and their effect on DEM error. The rougher the terrain, i.e. the steeper the slopes, the more difficult it is to measure elevation values. Elevation values located in close proximity will have similar terrain characteristics, and hence exhibit similar error properties.

While it is highly probable that errors in DEMs are correlated, information on the correlation is normally lacking from the accuracy information provided with the elevation data. The DEM used in this study was no exception. To investigate the effect of correlated error, a 21×21 kernel matrix consisting of values from a folded normal distribution was convolved with the DEM grid. The folded normal, with a standard deviation of 5 m and a mean of 0, was centred in the matrix so that the centre value had the largest weight, with cells farther away from having smaller weights. This agrees with the assumption that the closer the points, the more correlated the errors. The normal distribution is considered folded because it uses the distance from the centre point ($r^2 = x^2 + y^2$) as opposed to the x and y components individually. A standard deviation of 5 m was chosen for the folded normal since it created a distribution the fit the 21×21 kernel matrix well. However, without any knowledge of the correlation, any standard deviation value could have been used.

Convolution with a folded normal kernel successfully correlates the error; how-

ever, it has the undesirable side-effect of reducing the standard deviation of the entire matrix. Since the stated accuracy of the DEM was ±3 m, the error realisations of the DEM need to have a standard deviation of 3 m, regardless of its correlation. In order to maintain a standard deviation of 3 m after correlation, the initial uncorrelated matrices had to have a much higher standard deviation. The initial standard deviation required in order to produce a resulting standard deviation of 3 m can be determined by

$$\sigma_{initial} = \frac{\sigma_{final}}{\sqrt{\sum W^2}}, \tag{5.1}$$

where σ is the standard deviation, and W are the weights of convolution matrix. The weights of the convolution matrix are normalised to one ($\sum W = 1$). Based on Equation 5.1, the initial standard deviation of the uncorrelated error grids used so that the standard deviation of the error grids after correlation was 3 was determined to be 49.52.

In order to ensure that the convolution with a 21×21 folded normal did increase the correlation of an error grid, the autocorrelation function of both the uncorrelated and correlated error grids were found. The autocorrelation function of the uncorrelated error grid, as expected, only produced a spike at the centre of the distribution – confirming that the uncorrelated error grid is completely uncorrelated. The autocorrelation function of the correlated error grid, on the other hand, had a distinctive 2 dimensional bell shape curve. This indicated that the correlated error is indeed correlated with distance. For comparison, a horizontal cross section of the two autocorrelation functions is provided in Figure 5.2.

The method used to apply the Monte Carlo method of error propagation to cor-
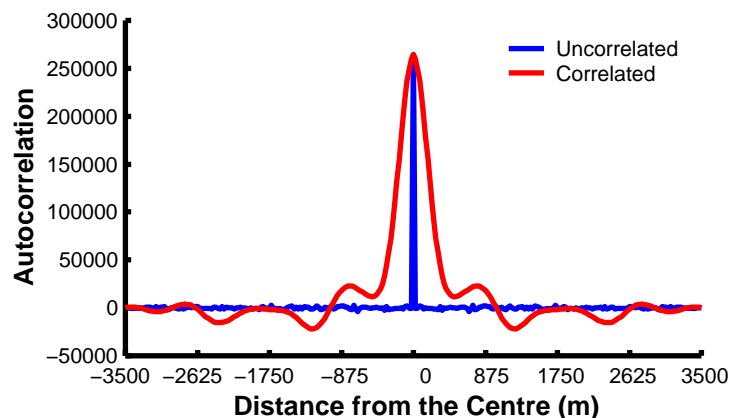
Figure 5.2: Horizontal cross section of the autocorrelation function (the correlation function is radially symmetric). Distances are based on a 25 m grid spacing.

related error is the same as that used for the uncorrelated error. The only difference is that the error grids need to be correlated before they are added to the original DEM. It should be noted that correlating the error does not effect the number of realisations required. A plot of the standard deviation of the standard deviation for correlated error is exactly the same as that shown in Figure 5.1. Therefore, as with the uncorrelated error, 500 realisations of the correlated error were used to examine the effect of correlated error on the calculation of topographic parameters.

5.2   Calculation of Topographic Parameters

Each of the 1000 error realisations – 500 uncorrelated and 500 correlated – was used to calculate grids of four different topographic parameters: slope, aspect, upslope area and the topographic index. Furthermore, eight different algorithms were used to calculate slope and aspect, and, depending on these algorithms, three different

algorithms were used to calculate upslope area. Outlined below are the specific topographic parameters along with the algorithms that were used.

5.2.1 Slope and Aspect

The primary topographic parameters associated with a DEM are slope and aspect. Other topographic parameters generally require calculation of these values first. Therefore, the method used to calculate the slope and aspect is important. Investigated in this study is the effect of DEM error on eight of the primary algorithms used to calculate slope and aspect that were introduced in Chapter 2. The algorithms include:

- Steepest Neighbour Algorithms
  - Maximum Downhill Gradient (MDG)
  - Maximum Adjacent Gradient (MAG)
  - Multiple Downhill Neighbours (MDN)
- Three Neighbour Algorithm
  - Three Point Plane (TPP)
- Four Neighbour Algorithms
  - Four Closest Neighbours (FCN)
  - Four Diagonal Neighbours (FDN)
- Eight Neighbour Algorithms
  - Eight Neighbours Unweighted (ENU)
  - One Over Distance Squared (OODS)

It should be recalled that the primary difference between these algorithms is the number of neighbours applied in the calculation.

All of the slope and aspect algorithms require knowledge of a cell's neighbours. This means that all of these algorithms experience problems at the edges of a DEM. Cells on the edge, by definition, have at least one neighbour that is undefined, i.e. outside the desired or known area. Therefore, it is impossible to perform any calculation that is based on knowledge of all eight neighbour without introducing a bias. Values at the edges can be found through modifications of the original algorithms, but this can introduce an unknown uncertainty into the models themselves. To avoid introducing additional model uncertainty, edge values in this study were ignored. The edges were used to calculate slope and aspect values, but values were not determined for the edges themselves. Ignoring the edges has the effect of 'shrinking' the watershed by one grid cell along its edge. Since all the information in the watershed was required for hydrological modelling, the watershed DEM used to determine the slope and aspect was expanded by one grid cell all around. By doing this, none of the information available for the watershed itself was lost.

5.2.2 Upslope Area

Aspect values of the watershed are used to calculate the upslope area for each grid cell in the watershed. The determination of upslope area essentially involves tracing the flow paths of water through a watershed to the drainage outlet. The algorithms available to calculate the upslope area compliment the algorithms used to calculate the slope and aspect, and were described in Chapter 2. The following is a list of the three upslope area algorithms used in this study along with the slope and aspect

algorithms that are used with them:

- Single Flow
  - MDG
  - MAG
- Multiple Flow
  - MDN
- Plane Fitting
  - TPP
  - FCN
  - FDN
  - ENU
  - OODS

An upslope area grid was determined for each realisation and for each slope and aspect algorithm. Since the ultimate goal was to find the topographic index value for each cell, and since the topographic index uses the upslope area in the form of the specific catchment area, the results for upslope area were expressed in terms of the specific catchment area (m instead of m^2). The only difference between the specific catchment area and the upslope area is that the specific catchment area is the upslope area divided by the grid size (25 m in this study).

5.2.3   Pit Removal

In order to determine the topographic index for each grid cell in the watershed, both the slope and upslope area must be defined everywhere. In addition, flow must be routed out of the watershed and not accumulate in localised areas. Problems occur

when the slope – and by extension the aspect – are undefined. This occurs in flat areas and, depending on the slope and aspect algorithm used, at closed depressions (pits). An undefined aspect becomes a problem when trying to calculate upslope area because there is no knowledge on how to route water out of a cell. Therefore, to get accurate values of upslope area, and to be able to create a topographic index grid that can be applied to a hydrological model, areas of undefined slope and aspect must be corrected.

In the watershed used in this study, there were only a few single cell pits. Therefore, only the problem of single localised pits was dealt with, and not the more complex problems associated with larger pits and flat areas. Because of the design of the algorithms studied, the only algorithms that had problems with these pits were those based on the steepest neighbour (MDG, MAG and MDN). The problems of pit removal in these algorithms could be further restricted to the problem of finding a method to route water through a pit using the MDG method, since the other two algorithms can be ultimately reduced to a form of this algorithm.

A simple way to handle pits is to manually remove them from the DEM before the calculation of topographic parameters. In this study this was not feasible because of the many error realisations. Adding error grids to the original DEMs to create error realisations had the effect of generating pits that were not present in the original DEM. Because of this, the pits had to removed after the creation of the aspect grids for each error realisation and could not just be removed from the original DEM.

The method employed to deal with pits essentially involved rerouting flow out of the pit. This required the initial creation of an aspect grid. From the aspect grid, those cells with undefined aspect values were selected. An example of a pit cell,

depicted in red, is shown in Figure 5.3(a). Once a pit was found it was assigned an aspect that corresponded to the direction to the neighbour with the lowest elevation. The flow path from this neighbour was then traced to ensure that it flowed out of the watershed. If the flow path did not leave the watershed, the aspect of the neighbour was changed to the direction of its next lowest neighbour. This process was repeated until a flow path was found that flowed out of the watershed. Reassignment of aspect was restricted to cells that were not already being rerouted. Using this method, only a few aspect values typically required modification. An example of a flow path reroute is shown in Figure 5.3(b).
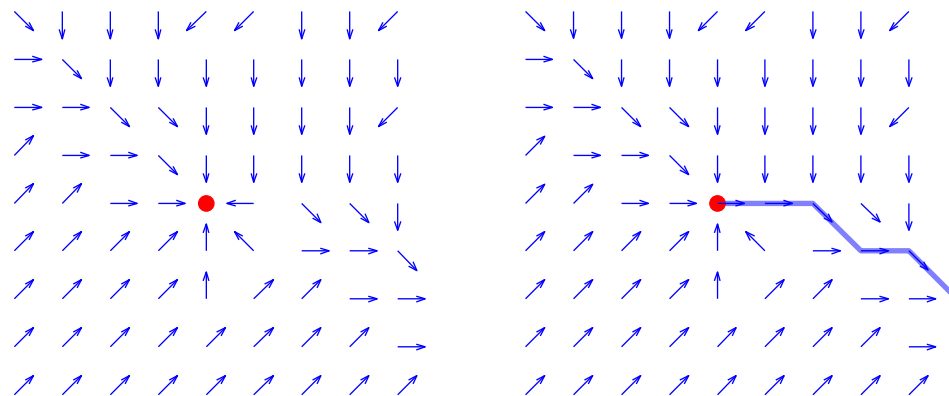
(a) Before pit correction.

(b) After pit correction with the new flow path marked in light blue.

Figure 5.3: Flow directions of cells using MDG before and after pit correction. Quiver lines represent the aspect direction and the red dot is the location of the pit.

Once the problem of an undefined aspect for pits has been addressed, the only problem remaining is that of an undefined slope. The slope for a flat area is, by definition, zero. Pits can also be viewed as flat because before there can be any

outflow from them, their water level must theoretically reach a height level with that of their lowest neighbour. However, in either case the zero slope value would create an undefined topographic index. Therefore, to avoid any undefined topographic indices, all flat grid cells, and by extension all pits in the watershed were assigned a very small value. This very small value was arbitrarily selected to be 0.000001.

5.2.4   The Topographic Index

Topographic index grids were calculated for each of the eight slope and aspect algorithms and for every error realisation of the watershed. The value of the topographic index for each cell in a realisation was found using the slope and corresponding upslope area grids. The topographic index for each grid cell was then found using Equation 3.1.

In order to conform to the input format required by the hydrological model TOP-MODEL the topographic index grids were converted into topographic index distributions. This was done by first finding the lowest and highest topographic index values. These values were used to determine the low and high limits of the distribution. The lowest value was rounded down to a value divisible by 0.5, while the highest value was rounded up. The grid values were then binned into 0.5 intervals between the two limits. The choice of using 0.5 as the bin size was somewhat arbitrary. However, care was taken so that the bin size did not result in either too many bins or bins that were too coarse. Once binned the topographic index values were ready for input into TOPMODEL.

5.3   Topmodel Implementation

Using the topographic index distributions, TOPMODEL was implemented for all the combinations of calibrated input, slope and aspect algorithms, and uncorrelated and correlated error realisations. For the two calibration methods (MDG and ENU), the only difference in the input between realisations was the topographic index distribution. All other input parameters remained the same for the comparisons between calibration methods.

For all tests, the following output data was collected from TOPMODEL:

- Estimated Hydrograph
- Total overland flow
- Total discharge
- Efficiency (EE)
- RMS error

As with the observed hydrographs, the estimated hydrographs exhibited two distinctive rain events. From the estimated hydrograph four values were extracted: the time to the two peaks and their heights. The times to peak were measured as the time delay, in hours, between the rain events and the discharge peaks.

5.4   Statistical Comparisons

Monte Carlo error simulation requires a statistical comparison of the results over all the realisations for a given method in order to produce comparable results. Specifically, the mean and standard deviation are required. As described in Section 5.1.1,

the mean represents the 'actual' value and the standard deviation is an indication of the variation or error in the value. For each type of gridded data (slope, aspect, upslope area and topographic index), the mean and standard deviation were calculated for each grid cell in the watershed over all the realisations of the different algorithms. These gridded mean and standard deviation values were then mapped to provide a visual representation of where the values have the most variation and over what type of terrain. In order to determine the error over the entire watershed for each of the topographic parameters, the mean and standard deviation over the mean grids was determined. This provided both the mean standard deviation and the variation in the standard deviation for each topographic parameter. These values were used to determine the effect of DEM errors on the topographic parameters. Comparison between the different algorithms lead to conclusions on which algorithms are more sensitive to error.

The realisation results from TOPMODEL can be analysed in a statistical fashion similar to that used with the topographic parameter grids. The primary difference in this case is that there are not any grids, just single values for each realisation. TOPMODEL results can be compared not only between algorithms, but also between calibration methods.

Chapter 6

Experimental Results

There are two primary objectives in this study: to investigate the effect of DEM error on four topographic parameters, and to investigate the effect of DEM error on the implementation of TOPMODEL. Therefore, the results of this study are divided into two sections reflecting the two primary objectives.

6.1   Topographic Parameters

For the four topographic parameters – slope, aspect, upslope area and topographic index – results were calculated using both uncorrelated and correlated DEM error. The results for each topographic parameter and algorithm are presented using overall error values along with error maps. The error maps are plots of the standard deviation values over all realisations for every cell in the watershed. For comparison, maps of the mean values at every grid cell are also provided. Overall error values are calculated as the mean standard deviation of the standard deviation grids for each slope and aspect algorithm and for both uncorrelated and correlated error. To show

how the mean standard deviation varies over the watershed, the standard deviation of the standard deviation maps is also given.

To avoid the presentation of an overwhelming number of plots, error maps are only given for topographic parameters that are based on the MDG and ENU slope and aspect algorithms. These two methods can be seen as two extremes in the investigated algorithms. MDG is based on a selection process that uses only one neighbour to calculated slope and aspect, and is the method most often used in hydrology. ENU, in contrast, uses all eight neighbours in the calculation of slope and aspect. This method has also been shown to produce slope and aspect values that more closely approximate those of the terrain (Skidmore, 1989; Guth, 1995). Furthermore, as will be shown in the results below, these two algorithms normally exhibit the highest (MDG) and lowest (ENU) error sensitivity, making them the logical choice for comparison. Except for the topographic index, error maps were only generated for the simulations performed using uncorrelated error. Correlating the error basically smoothes the error, reducing its effect. Therefore, the correlated error maps are similar to the uncorrelated error maps, and differ only in the magnitude of the error and in the extent of high error regions. The error map based on correlated error is, however, provided for topographic index because the calculation of it requires all of the other topographic parameters determined in the study. Consequently, it nicely summarises the cumulative effect of the error.

6.1.1 Slope

The overall effect of both uncorrelated and correlated DEM error on the calculation of slope is presented in Table 6.1. From these results a number of observations can be

made not only between the eight algorithms but also between the two types of error. All eight algorithms are, as expected, much less sensitive to correlated error than they are to uncorrelated error. This is understandable since all the algorithms are based on local neighbour operations, and correlating the error reduces the variation in local neighbourhoods. In other words, the error in a local neighbourhood will be more of an elevation bias and will hence will have less of an impact on the resulting slope value. Another interesting observation regarding correlated error is that correlating the error reduces the variation between algorithms. The mean standard deviation for uncorrelated error ranges between 0.1495 and 0.0483, while for correlated error the mean standard deviation only ranges between 0.0182 and 0.0164. Therefore, all eight slope algorithms are about equally sensitive to correlated error. Again, the reason is that the correlated error results in an elevation bias. Because none of the slope algorithms use the absolute elevation values, this bias does not effect their calculation.

While the errors in slope for the eight algorithms are fairly uniform for correlated error, the differences between algorithms are much larger for uncorrelated error. A general trend is that the more neighbours used in the calculation of slope, the less sensitive the result is to uncorrelated error. The errors in the steepest neighbour algorithms are, in general, larger then those of the four neighbour algorithms, which are in turn larger then those of the eight neighbour algorithms. This relationship is understandable since the more neighbours involved in the algorithm, the less likely the slope values will be affected by one, or a few, highly erroneous elevation values in neighbouring cells. Since the MDN algorithm calculates slope based on an average of all downslope neighbours, it is also reasonable that it is less sensitive to error then

Table 6.1: Mean and standard deviation of the standard deviation of slope for the entire watershed.

Error	Algorithm	Mean Standard Deviation	Standard Deviation of Standard Deviation
Uncorrelated	MDG	0.1325	0.0144
	MAG	0.1013	0.0110
	MDN	0.0785	0.0105
	TPP	0.1495	0.0250
	FCN	0.0817	0.0053
	FDN	0.0588	0.0030
	ENU	0.0483	0.0022
	OODS	0.0512	0.0024
Correlated	MDG	0.0180	0.0008
	MAG	0.0179	0.0008
	MDN	0.0164	0.0086
	TPP	0.0182	0.0006
	FCN	0.0176	0.0006
	FDN	0.0174	0.0006
	ENU	0.0175	0.0006
	OODS	0.0175	0.0006

the other steepest neighbour algorithms and even the FCN algorithm.

An apparent variation to this trend is the TPP method, which had the largest error of all the algorithms. However, this algorithm can be viewed as the algorithm that uses the least number of neighbours, and the algorithm most sensitive to the orientation of the grid. Even though the steepest neighbour algorithms only use one (or more then one as is the case in MDN) neighbour to calculate slope, they do take into account the other eight neighbours in the selection process. The TPP method, on the other hand, only uses two specific neighbours, not taking into account the other six in any way. This limitation can makes this method more vulnerable to highly erroneous elevation values.

Based on the significant differences in slope error between the FCN and FDN methods, along with the differences in slope error between the ENU and OODS methods, it is assumed that this watershed suffers from a grid orientation bias. That is, over the entire watershed, slopes are more dominant in the diagonal directions than they are in the cardinal directions, and consequently, the diagonal direction is less sensitive to error then the cardinal direction. This is evident by the error in the FDN slope algorithm being smaller then the error in the FCN slope algorithm, and also in the error in the ENU algorithm being smaller than the error in the OODS algorithm. In the ENU algorithm all eight neighbours are weighted the same, where as in the OODS algorithm the diagonal neighbours are weighted less then the cardinal neighbours. This essentially results in, for this particular watershed, the more erroneous neighbours having a more significant role in the determination of slope, resulting in a higher error sensitivity. The significance of the differences between the overall error in the FCN and FDN slope algorithms, as well as between the ENU and OODS slope algorithms, was statistically confirmed using a student's t-test.

While there has been little to no research into the error sensitivity of slope algorithms, there has been some research into the ability of these algorithms to accurately determine the 'true' values of slope (Guth, 1995; Jones, 1998; Skidmore, 1989; Veregin, 1997; Quinn et al., 1991). Regardless, the results of these studies are similar to the results found in this study – the more neighbours used in a slope algorithm the more accurately the slope values agreed with the actual value of slope. The steepest neighbour algorithms tended to produce the worse results, while the ENU and FCN algorithms tended to produce the best results.

To obtain an understanding of the structure of slope error in the watershed, error

maps for the MDG and the ENU methods using uncorrelated error were created and are shown in Figure 6.1.1. In order to determine if the value of slope plays a role in the amount of error, both mean slope maps (Figures 6.1(a) and 6.1(c)) and standard deviation slope maps (Figures 6.1(b) and 6.1(d)) were generated. From the mean slope maps it is apparent that the MDG method, on average, produces higher slope values then the ENU method. The mean value over the entire grid for the former was 0.446, while for the latter it was 0.406. This is a significant difference (confirmed using a student's t-test); however, similar results were obtained by Guth (1995), who found that the MDG method, and by extension the MAG method, tended to give significantly steeper slopes, especially in steep terrain. Though the mean slope values at each cell are different between the two methods, the overall slope pattern is similar.

Although the mean slope maps are generally similar, the differences in the standard deviation maps are evident. The error in slope for the ENU method is, for the most part, uniform across the watershed. An exception is a small region near the upper right hand edge of the watershed that is noticeably less sensitive to error. This region has a particularly low slope, which leads to the conclusion that areas of low slope are less sensitive to error. This confirms the research done by Veregin (1997). For the MDG method it is evident that the terrain is reflected in the error map. Hence, the error from this algorithm is more dependant upon the actual slope value. Like the ENU method, areas of low slope are less sensitive to error. However, in general, the error sensitivity for the MDG method is much higher then the error sensitivity for the ENU method across the entire watershed. The observation that areas of low slope are less sensitive to error is confirmed in Figure 6.2, which is a

(a) Mean slope using MDG.

(b) Standard deviation of slope using MDG.

(c) Mean slope using ENU.

(d) Standard deviation of slope using ENU.
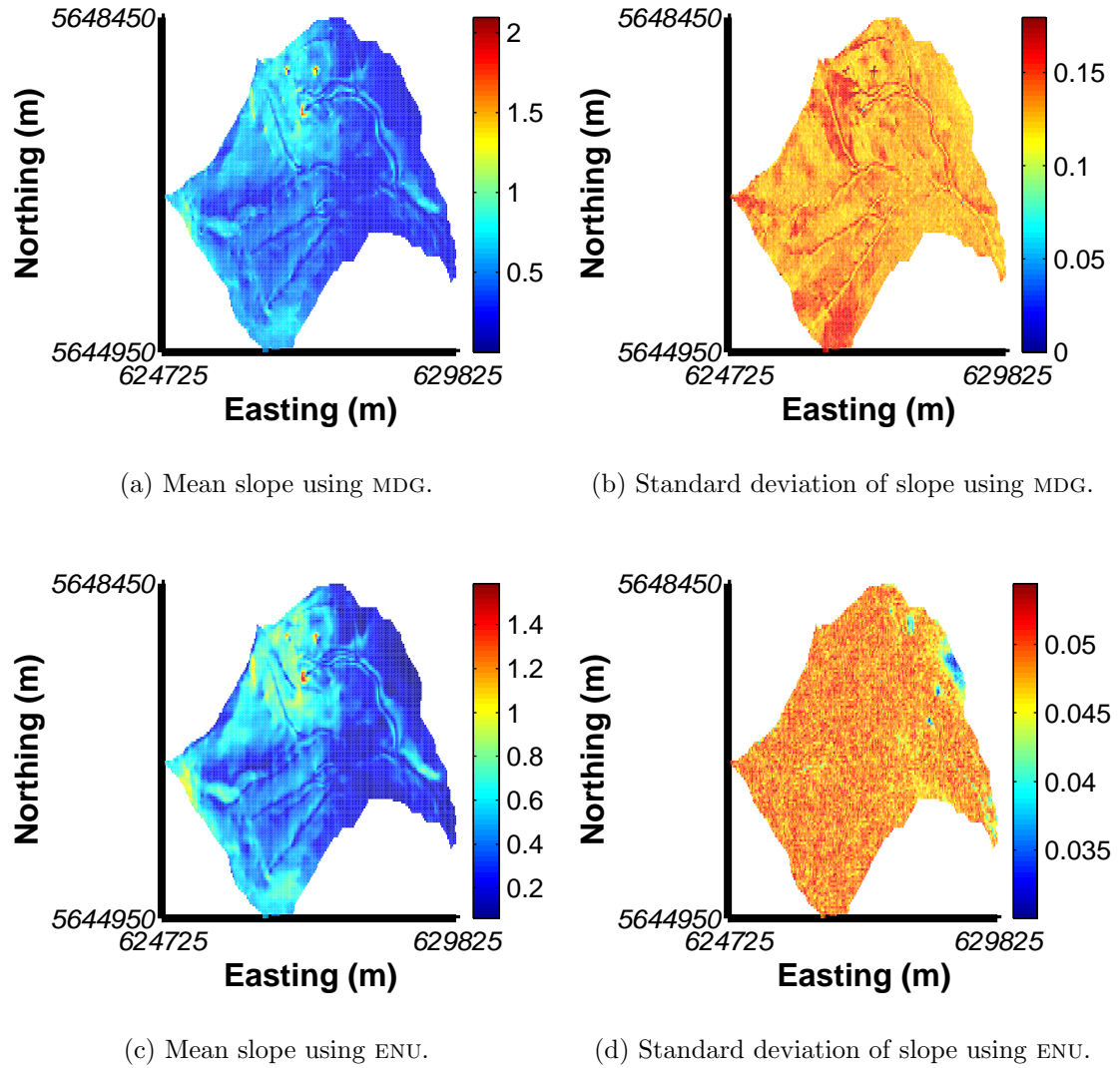
Figure 6.1: Slope error maps for uncorrelated error. The mean and standard deviation are determined for each cell over the 500 realisations.

plot of the standard deviation of slope as a function of the mean slope.
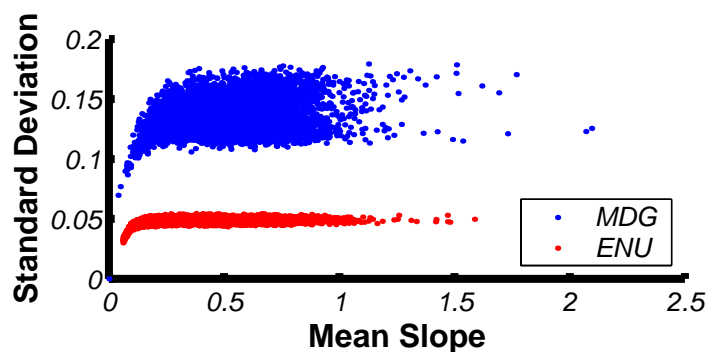
Figure 6.2: The standard deviation of slope as a function of the mean slope for each cell in the watershed for uncorrelated DEM error.

6.1.2   Aspect

The overall errors in aspect are presented in Table 6.2. These results exhibit relationships that are different to those observed for slope. Unlike the errors in slope, the errors in aspect (reflected in the mean standard deviation) do not appear to improve significantly when the DEM error is correlated. In some instances, the error sensitivity of aspect with the correlated error is even higher then it is with the uncorrelated error. In any case, however, the difference in error sensitivity between algorithms or between uncorrelated or correlated DEM error is almost always small. With the exception of correlated MDN, all mean standard deviation values lie within two degrees of 45°. While this might seem like a large amount of error, it only represents a displacement of one grid cell. Therefore, from these results it can be concluded that all eight algorithms are, essentially, equally sensitive to error, regardless of the form of the error (i.e., whether or not the error is correlated or uncorrelated).

Table 6.2: Mean and standard deviation of the standard deviation of aspect for the entire watershed.

Error	Algorithm	Mean Standard Deviation (degrees)	Standard Deviation of Standard Deviation (degrees)
Uncorrelated	MDG	44.39	16.35
	MAG	44.47	16.35
	MDN	43.67	16.25
	TPP	44.89	20.12
	FCN	44.05	30.07
	FDN	43.64	34.02
	ENU	43.72	36.47
	OODS	43.76	35.90
Correlated	MDG	43.70	65.98
	MAG	43.62	65.36
	MDN	50.28	60.80
	TPP	44.91	48.25
	FCN	44.73	46.39
	FDN	44.43	46.64
	ENU	44.52	46.40
	OODS	44.58	46.36

Aspect error maps for the MDG and ENU methods are presented in Figure 6.1.2. From the mean aspect maps (Figures 6.3(a) and 6.3(c)), it can be seen that there is little difference in the aspect values between the two algorithms. The only apparent difference between them is that the ENU plot is smoother. This is understandable since the MDG method is restricted to aspect values that are in 45°intervals, while the aspect values for the ENU method can be anything, resulting in smoother transitions.

The standard deviation maps for both algorithms (Figures 6.3(b) and 6.3(d)) are similar to each other. This is not unexpected, because both algorithms have similar overall error values. Error is fairly constant across the watershed for both algorithms. Error tends to be a little higher for MDG then for ENU in the lower slope areas and along the drainage network, but this variation is not as large as that seen in slope errors. For both algorithms the area of highest aspect error is located in the same location as the area of lowest error for slope, i.e., the upper right hand edge. As shown in Figure 6.1.1, this is a low slope area. It is understandable that areas of low slope are also areas of high aspect error since a small error in slope can dramatically affect the aspect. An important observation that can be made about the aspect error is that its magnitude is not dependent on the aspect value itself, but is more related to the value of slope. This can be seen by comparing Figures 6.4 and 6.5, which plot the standard deviation of aspect as a function of the mean aspect and slope values respectively. From these plots its is apparent that aspect error is correlated with slope and not aspect.
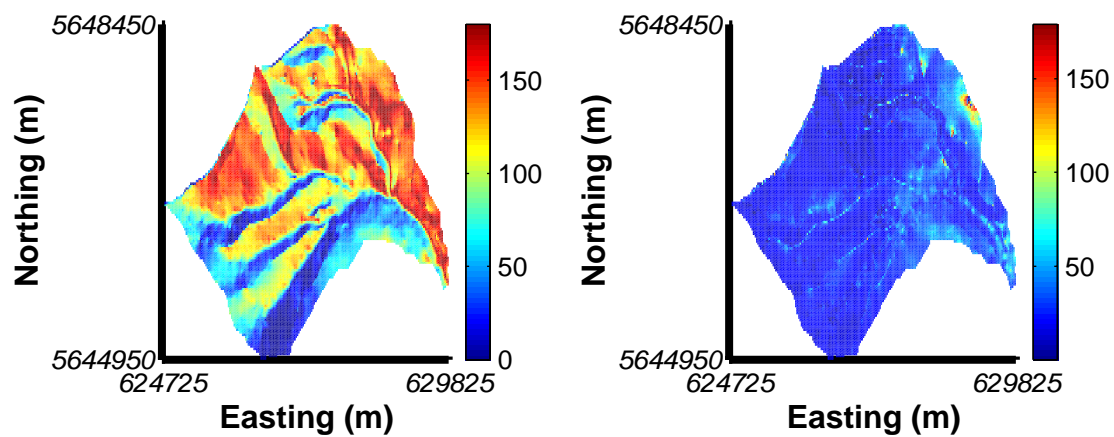
(a) Mean aspect using MDG.

(b) Absolute Standard deviation of aspect using MDG.
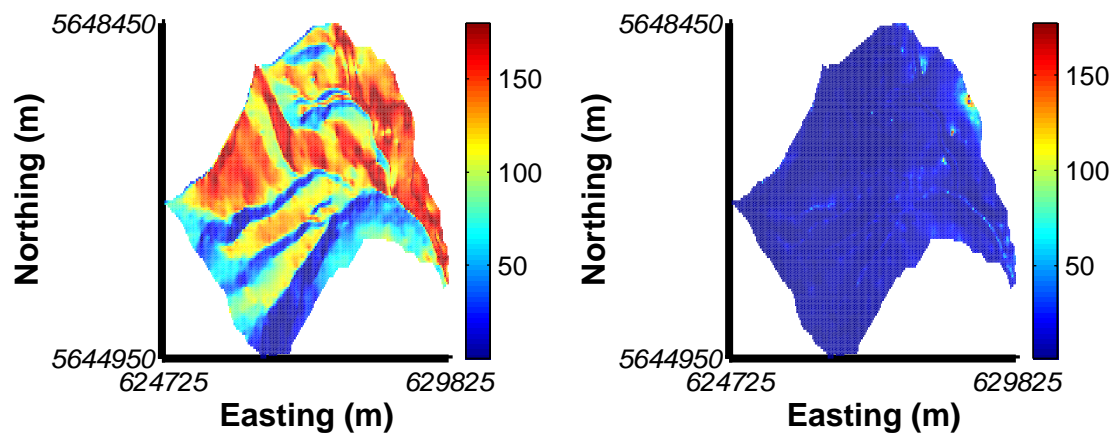
(c) Mean aspect using ENU.

(d) Absolute Standard deviation of aspect using ENU.

Figure 6.3: Aspect error maps for uncorrelated error. The mean and standard deviation are determined for each cell over the 500 realisations. Aspect values are expressed in degrees.
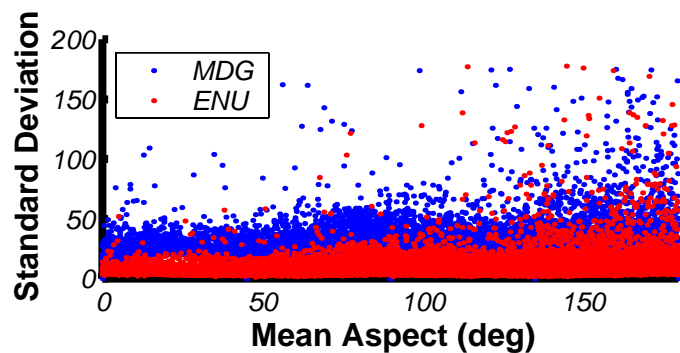
Figure 6.4: The standard deviation of aspect as a function of the mean aspect for each cell in the watershed for uncorrelated DEM error.
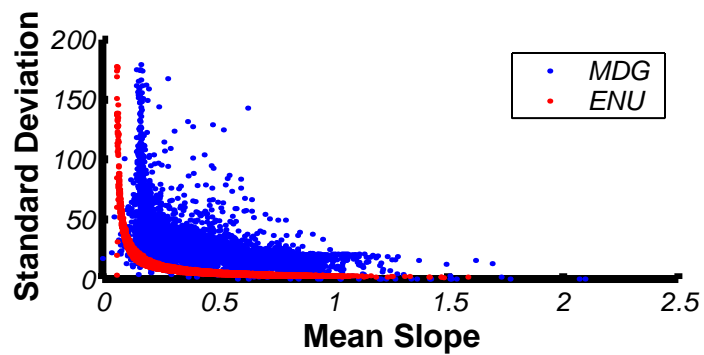
Figure 6.5: The standard deviation of aspect as a function of the mean slope for each cell in the watershed for uncorrelated DEM error.

6.1.3   Upslope Area

From the aspect values for each realisation, error type, and slope and aspect algorithm, upslope area maps were generated. The overall errors in upslope slope area are given in Table 6.3. From these results it is apparent that, as was found for slope errors, all eight algorithms are less sensitive to correlated error then they are to uncorrelated error. The reasons for this are similar to those given for slope (Section 6.1.1). However, unlike the errors in slope, correlating the DEM error does not reduce the variation in error between the algorithms. This difference from the slope results can be attributed to the difference between global and neighbourhood operations. Slope, as calculated in this study, is restricted to neighbourhood operations, and, hence, treats correlated error as a bias. Upslope area, on the other hand, is more of a global operation, and hence is affected by values outside the region of correlation.

The overall error between the eight slope and aspect algorithms, for both uncorrelated and correlated DEM error, appears to follow two patterns. These two patterns correspond to the two distinctive types of algorithms: those based on the steepest neighbour, and those that are not. For the algorithms based on the steepest neighbour principle, it is apparent that the smaller the dependence on a single steepest neighbour, the smaller the sensitivity to DEM error. The MDG algorithm, which is based entirely on a single steepest neighbour has the larger error, while the MDN algorithm, which uses all downslope neighbours, has the lowest error. Based on the way the upslope area is calculated for these two algorithms, this result is understandable. The MDG algorithm only allows single cell flow – flow from one cell flows completely into a single neighbouring cell. Since the flow is never divided, it is difficult for this method to 'recover' from erroneous elevation values. If the flow is misdirected for a

Table 6.3: Mean and standard deviation of the standard deviation of upslope area for the entire watershed.

Error	Algorithm	Mean Standard Deviation (m)	Standard Deviation of Standard Deviation (m)
Uncorrelated	MDG	4314.49	18212.98
	MAG	797.12	1613.58
	MDN	151.79	464.93
	TPP	87.22	147.99
	FCN	180.34	526.34
	FDN	226.99	732.47
	ENU	253.50	741.65
	OODS	264.83	793.60
Correlated	MDG	1099.26	8465.67
	MAG	615.43	2189.31
	MDN	281.52	1391.18
	TPP	98.85	369.43
	FCN	133.28	689.04
	FDN	175.00	774.27
	ENU	151.80	657.34
	OODS	143.80	667.55

specific cell in a given realisation by even one grid cell, there is little to no chance that the flow will follow the same path as that in another realisation. Since upslope area of one grid cell is connected to the upslope area of the other cells in the watershed, errors compound downslope. For the MDN algorithm flow is divided between all downslope neighbours. It is therefore possible for flow to diverge and converge as it travels downslope. Because of this, the variation in upslope area for each grid cell will be less then that observed using the MDG algorithm. The reason that the MAG algorithm is less sensitive to error than the MDG algorithm, even though it is also based on a single neighbour, is that it finds the neighbour with the maximum slope, not just the neighbour with the maximum downslope. Therefore, this method has a greater ability to choose the 'correct' flow direction. However, the MAG method is still limited by the same factors affecting the MDG method, and therefore it has a sensitivity to error that is larger than that of the MDN method.

The five remaining slope and aspect algorithms (TPP, FCN, FDN, ENU and OODS) exhibit an error pattern that can be viewed as the opposite of that seen for the steepest neighbour based algorithms. For these remaining algorithms, the error in upslope area increases with an increase in the number of neighbours used in the algorithm. All of these methods calculate upslope area in a similar manner using plane fitting. Therefore, the only difference between the algorithms is the number of neighbours used to determine aspect. None of these methods placed any restrictions on aspect values, i.e., aspect was not limited to 45°bins. Since the error in aspect was found to be fairly constant between algorithms, and if anything was slightly larger in algorithms that use fewer neighbours, the results obtained for upslope area are a little baffling.

Comparing the two mean upslope area plots (Figures 6.6(a) and 6.6(c)) it is clear that the MDG method produces a visible drainage network with a definable outflow location, while the ENU method does not. The determination of upslope area is normally done with the goal of extracting a drainage network. Except for a few disconnected lines, the ENU method does not appear to accomplish this goal. Similar poor connectivity is observed in all the algorithms that are not based on the steepest neighbour principle. Furthermore, as the number of neighbours used in an algorithm decreases, the more disconnected the drainage network becomes. Or, alternatively, the fewer neighbours used in an algorithm, the more uniform the upslope area values are across the watershed. If the upslope area is relatively uniform across the watershed, then it is less likely that there will be any variation in a single cell's value between realisations. If, on the other hand, there are distinctive features that have widely different values, there is a greater opportunity for variation over realisations. It is therefore understandable that, for slope and aspect algorithms not based on the steepest neighbour, the overall error in upslope area will increase with the number of neighbours involved. In other words, the fewer the neighbours, the more uniform the upslope area, and the more uniform the upslope area, the smaller the variation between realisations. For those algorithms not based upon the steepest neighbour principle, this explains the observed rise in upslope area error as the number of neighbours increased.

From the two standard deviation plots (Figures 6.6(b) and 6.6(d)), it can clearly be seen that the greatest error in upslope area occurs along the drainage network. The drainage network is the location of high upslope area values. Therefore, a large error is associated with a large upslope area. This relationship is shown in Figure 6.7,

(a) Mean upslope area using MDG.

(b) Standard deviation of upslope area using MDG.

(c) Mean upslope area using ENU.

(d) Standard deviation of upslope area using ENU.
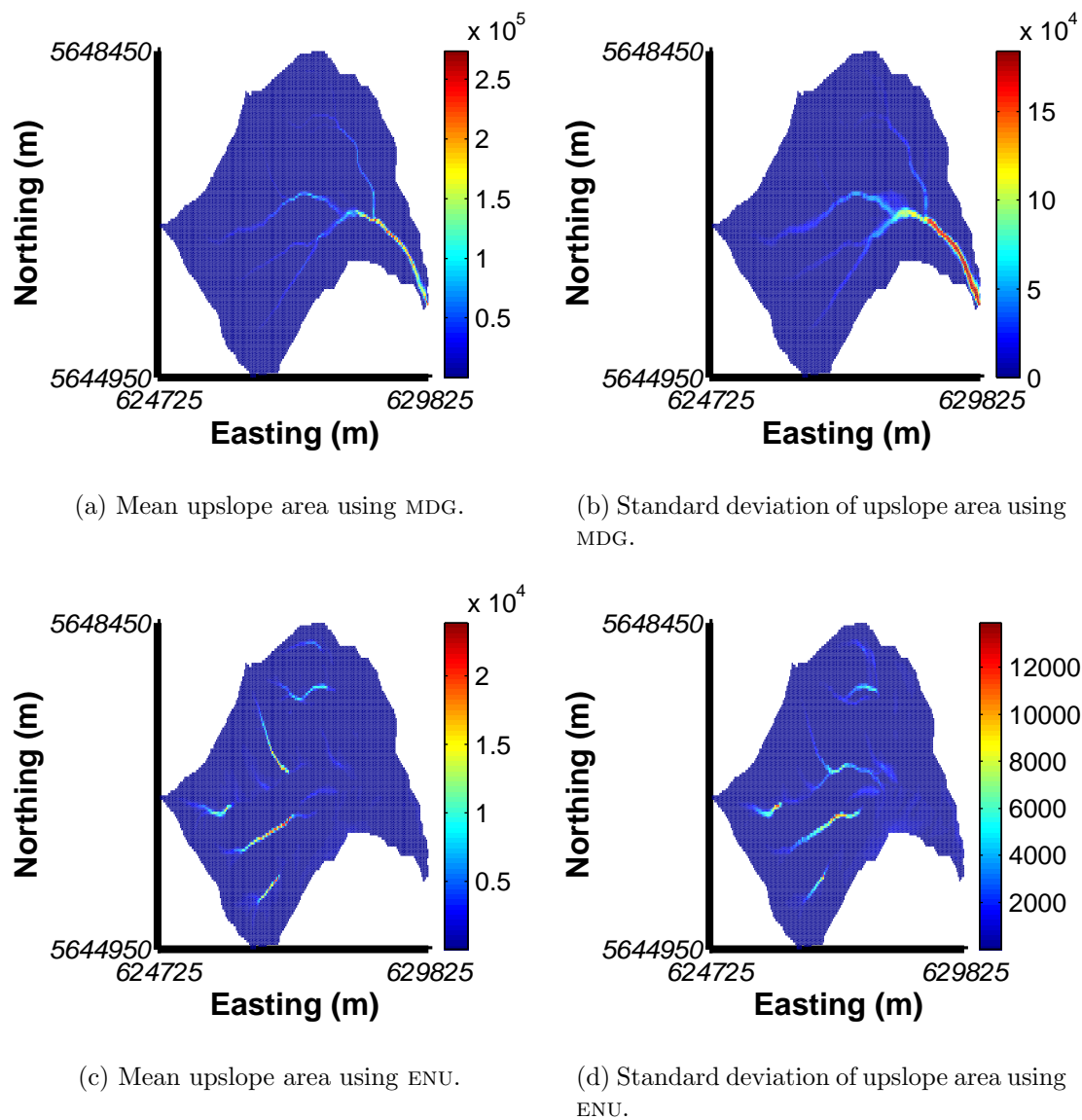
Figure 6.6: Upslope area error maps for uncorrelated error. The mean and standard deviation are determined for each cell over the 500 realisations. Upslope area values are expressed in metres.

where the standard deviation of upslope area for each cell in the watershed is plotted as a function of the mean. As stated before, upslope area is an accumulation process and errors will tend to compound as the size of the upslope area is increased. Since the drainage networks represent locations of flow accumulation, it is reasonable to expect these regions to be more susceptible to error. The largest error for the MDG method is, as expected, at the drainage outlet. Upslope area errors are generally larger for the MDG method as opposed to the ENU method across the watershed, and this is especially noticeable along the drainage networks.

An unusual phenomenon can be observed in Figure 6.7 for the upslope area calculated using the MDG method. Three distinct curves are visible, each with a different maximum error value. These different curves likely correspond to data from different geographic locations in the watershed, i.e. along the different branches of the drainage network. As observed before, flatter areas tend to be more sensitive to error. It stands to reason therefore, that drainage networks from flatter areas will in general experience less upslope area error sensitivity than drainage networks from steeper areas. Since the upslope area errors for the ENU method were so small, and since the drainage network was not very well defined for this method, this method did not exhibit the curve differences observed for the MDG method.

6.1.4 Topographic Index

The last topographic parameter investigated was the topographic index. The overall effect of uncorrelated and correlated DEM error on the eight algorithms used to calculated the topographic index are presented in Table 6.4. The patterns observed for errors in the topographic index between algorithms and between uncorrelated
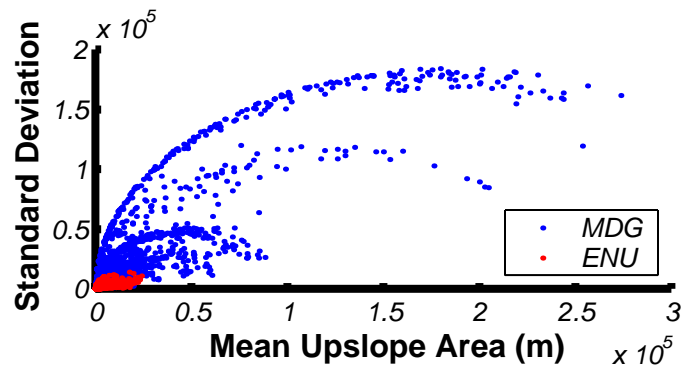
Figure 6.7: The standard deviation of upslope area as a function of the mean upslope area for
each cell in the watershed for uncorrelated DEM error.

and correlated error are a combination of those observed for both slope and upslope

area. The differences in the overall topographic index errors between uncorrelated

and correlated DEM error are similar to those exhibited by the upslope area. That

is, correlated DEM error reduces the amount of error in the topographic index for

all eight algorithms, but it does not equalise the error sensitivity as it does for

slope. However, like slope, the topographic index error decreases with an increase in

the number of neighbours utilised in the algorithm. However, unlike for slope, the

steepest neighbour algorithms (MDG, MAG and MDN) all suffer from a larger error

then the other algorithms. This observation includes the TPP method, which (again,

unlike slope) has a smaller error than all of the steepest neighbour algorithms. The

reason for this difference is related to the large error in upslope area found in the

steepest neighbour algorithms. Another similarity between slope and topographic

index error is the apparent grid orientation bias. The explanations for the observed

patterns in topographic index error are the same as those given for the errors in slope

and upslope area.

Table 6.4: Mean and standard deviation of the standard deviation of topographic index for the entire watershed.

Error	Algorithm	Mean Standard Deviation	Standard Deviation of Standard Deviation
Uncorrelated	MDG	1.9297	1.1937
	MAG	1.2218	0.4562
	MDN	1.2392	0.8833
	TPP	0.7970	0.2647
	FCN	0.7022	0.3602
	FDN	0.5841	0.3909
	ENU	0.5783	0.4060
	OODS	0.6112	0.4129
Correlated	MDG	0.4559	0.4658
	MAG	0.4774	0.4638
	MDN	0.3975	0.4658
	TPP	0.2883	0.3789
	FCN	0.2551	0.3529
	FDN	0.2330	0.3146
	ENU	0.2342	0.3294
	OODS	0.2360	0.3395

Topographic index error maps for the MDG and ENU methods are presented in Figure 6.1.4. Like the overall error discussed above, the mean (Figures 6.8(a) and 6.8(c)) and standard deviation maps (Figures 6.8(b) and 6.8(d)) have attributes similar to those seen in the error maps for slope and upslope area (Figures 6.1.1 and 6.1.3 respectively). By comparing the two mean topographic index maps it is apparent that the MDG method, on average, produces higher values then the ENU method. While a drainage network is visible in the mean plots for both methods, the one produced using the MDG method is more highly defined. These observations were also made for the mean maps for slope and upslope area.

The standard deviation maps for the MDG and ENU algorithms have appearances that have already been described by the error maps of slope and upslope area. For both algorithms, the drainage network is visible in the error maps, but is more prominent for the MDG algorithm. Error for both methods is greatest along the drainage network and in areas of low slope. Topographic error are, in general, larger for the MDG method than the ENU method across the entire watershed.

To compare the error maps generated using uncorrelated and correlated DEM error, the topographic index error maps resulting from correlated error were created for the MDG and ENU algorithms, and are shown in Figure 6.1.4. For both algorithms there is very little difference visible between the mean plots for the uncorrelated error and the mean plots for the correlated error. This is reflected in the small average differences in the mean topographic index values between the two types of error simulations. For the MDG algorithm the difference was 0.63, and for the ENU algorithm it was an even smaller 0.33. The difference between error types is, however, much more significant when the standard deviations are examined. This is because

(a) Mean topographic index using MDG.

(b) Standard deviation of topographic index using MDG.

(c) Mean topographic index using ENU.

(d) Standard deviation of topographic index using ENU.
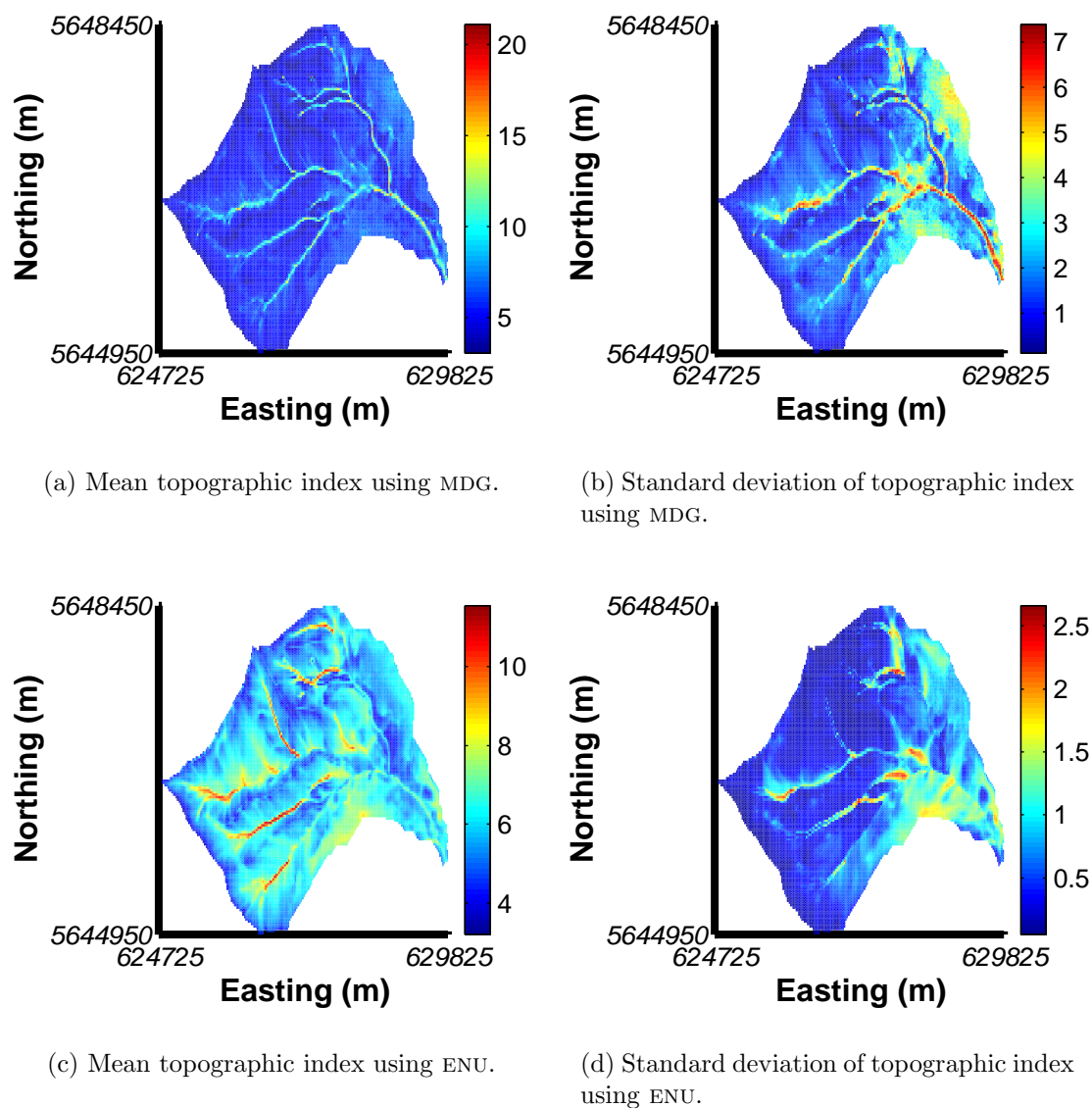
Figure 6.8: Topographic index error maps for uncorrelated error. The mean and standard deviation are determined for each cell over the 500 realisations.

correlated error significantly reduces the error sensitivity of both algorithms. While features visible in the topographic index error plots generated using uncorrelated error are visible in the error plots generated using correlated error, correlated error does tend to make the error more uniform across the watershed. Therefore, while correlated DEM error does not affect the value of topographic index, it does reduce the error sensitivity.

The form of the topographic index required for input into TOPMODEL is a binned distribution. The mean topographic distribution for the eight algorithms generated using uncorrelated DEM error are presented in Figure 6.1.4. For comparison, the two distributions used to calibrate TOPMODEL are also included. All distribution functions have been binned at 0.5 intervals. To emphasise the differences in the prominent part of the distributions, the scale on the x-axis has been truncated at 15 for all plots. While most distributions terminate before a topographic index value of 15, there are a few that do not. Those include MDG Calibration (max = 27.5), MDG (max = 22) and MDN (max = 20). From the mean topographic distribution plots it can be seen that, as expected, similar algorithms produce similar distributions.

The mean, standard deviation and skewness for the topographic distributions are provided in Table 6.5. Both the mean, and especially the skewness of the distributions, will play a significant role in describing the TOPMODEL results. From Table 6.5 it can be seen that correlated error tends to equalise the means of the distributions and reduce the skewness when compared to uncorrelated DEM error. Between algorithms it appears that those based on the steepest neighbour are more skewed than those based on the other algorithms. Between the other algorithms it appears that the more neighbours used in the determination of the slope and aspect the more

(a) Mean topographic index using MDG.

(b) Standard deviation of topographic index using MDG.

(c) Mean topographic index using ENU.
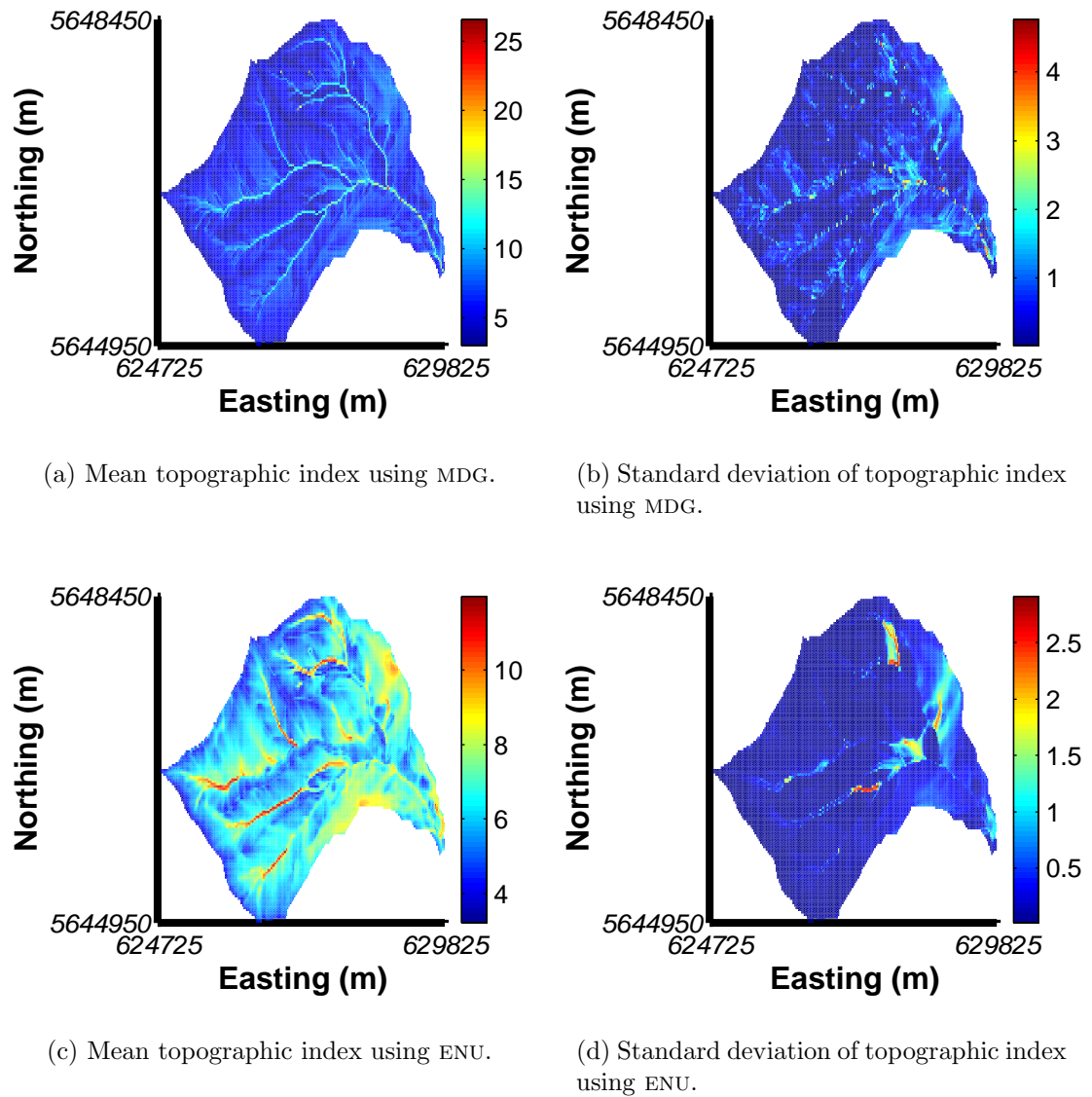
(d) Standard deviation of topographic index using ENU.

Figure 6.9: Topographic index error maps for correlated error. The mean and standard deviation are determined for each cell over the 500 realisations.
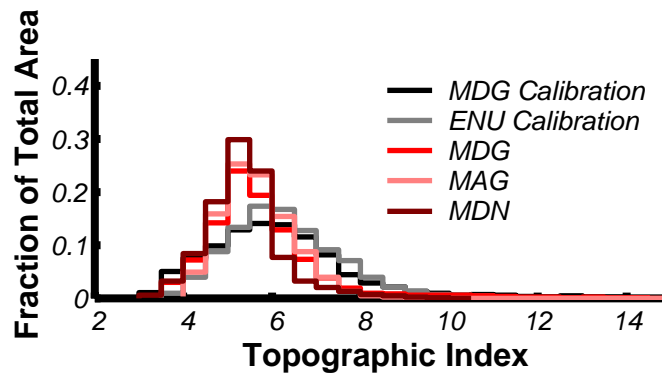
(a) Steepest Neighbour Algorithms
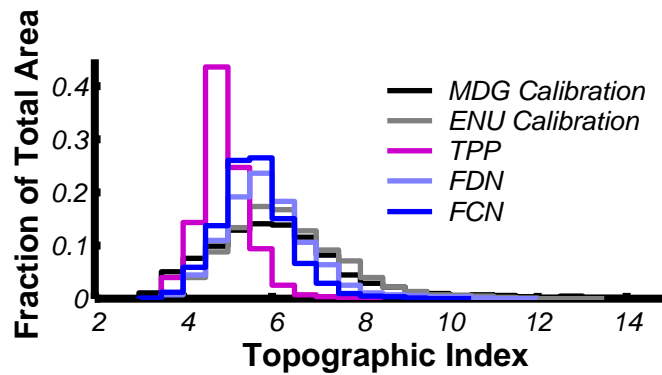
(b) Three and Four Neighbour Algorithms
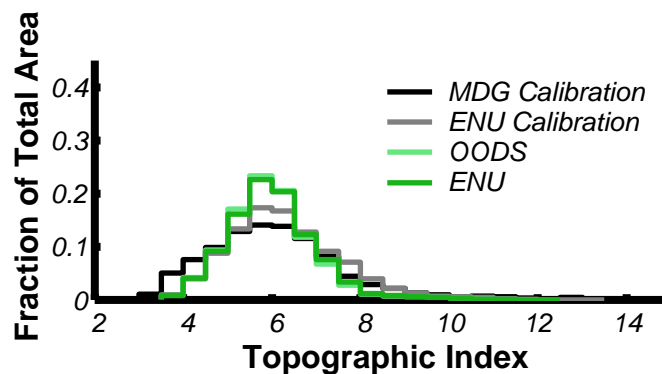
(c) Eight Neighbour Algorithms

Figure 6.10: Mean topographic index distributions for the eight slope and aspect algorithms using uncorrelated error. The two TOPMODEL calibration distributions are provided for comparison.

skewed the topographic distribution. These observations coincide with the ability of an algorithm to resolve a drainage network.

Table 6.5: Characteristics of the mean topographic index distributions.

Error	Algorithm	Mean	Standard Deviation	Skew
Uncorrelated	MDG	6.04	4.54	1.17
	MAG	5.63	2.21	0.62
	MDN	5.91	2.22	0.86
	TPP	5.16	1.34	0.44
	FCN	5.85	2.04	0.45
	FDN	6.16	2.73	0.60
	ENU	6.28	2.83	0.59
	OODS	6.22	2.71	0.58
Correlated	MDG	6.45	5.41	1.10
	MAG	6.33	3.95	0.53
	MDN	6.45	4.09	0.80
	TPP	6.32	2.86	0.29
	FCN	6.50	3.20	0.43
	FDN	6.61	3.37	0.46
	ENU	6.60	3.37	0.46
	OODS	6.59	3.37	0.46

6.2   Topmodel

The effect of DEM error on the results of TOPMODEL was investigated for the eight slope and aspect algorithms of the previous section. However, before TOPMODEL could be used effectively it first required calibration. This, in turn, required a topographic index distribution generated using one of the eight algorithms. To eliminate any bias towards the algorithm used for calibration, TOPMODEL was calibrated twice with two different algorithms – MDG and ENU. The results from these calibrations

were then used in a Monte Carlo simulation for each of the eight slope and aspect algorithms, and for both uncorrelated and correlated error. As for the previous tests, each Monte Carlo simulation used 500 realisations.

Aside from generating a hydrograph for the desired time series, TOPMODEL also provides statistics that compare its estimated hydrograph to the observed hydrograph. For this study, the hydrographs produced during calibration (one for MDG calibration and one for ENU calibration) were used as the observed hydrograph during later testing. The two statistics presented include the efficiency (EE) and the root mean square (rms) error. An efficiency value of 1.0 indicates a perfect fit, and the closer the efficiency is to 1.0 the more the estimated hydrograph resembles the observed. A small rms error value is also an indication of a good fit. The statistics for the eight algorithms and the two types of DEM error for both MDG and ENU calibration are provided in Tables 6.6 and 6.7 respectively. In these tables the statistics are presented as the mean and standard deviation over all 500 realisations.

The statistics for the two types of calibration have some similar properties. For both calibrations, the correlation of DEM error tends to increase the average fit of the estimated hydrograph to the calibrated hydrograph. Whether or not correlation reduces the variance in the fit is dependent on the algorithm and calibration method. However, the variation is, in general, fairly small. Not surprisingly, for each calibration method the algorithm that produced the best fit and had the least amount of variation was the method initially used for the calibration. Additionally, algorithms that more closely resembled those used for calibration also tended to perform better. This is understandable since similar algorithms tend to produce similar topographic distributions. Attention should be drawn to the very poor results from the TPP

Table 6.6: Statistics comparing the TOPMODEL estimated hydrographs calibrated using the MDG topographic distribution to the MDG calibrated hydrograph.

Error	Algorithm	Efficiency		RMS Error (10^{-6})	
		Mean	Standard Deviation	Mean	Standard Deviation
Uncorrelated	MDG	0.921	0.014	1.18	0.50
	MAG	0.598	0.058	2.67	1.01
	MDN	0.566	0.080	2.78	1.19
	TPP	-0.050	0.011	4.32	0.45
	FCN	0.157	0.060	3.87	1.03
	FDN	0.490	0.066	3.01	1.08
	ENU	0.576	0.061	2.75	1.04
	OODS	0.535	0.070	2.88	1.11
Correlated	MDG	0.996	0.004	0.27	0.26
	MAG	0.967	0.016	0.77	0.553
	MDN	0.864	0.156	1.56	1.66
	TPP	0.225	0.072	3.71	1.13
	FCN	0.553	0.068	2.82	1.10
	FDN	0.713	0.055	2.26	0.99
	ENU	0.709	0.055	2.28	0.99
	OODS	0.709	0.054	2.28	0.98

Table 6.7: Statistics comparing the TOPMODEL estimated hydrographs calibrated using the ENU topographic distribution to the ENU calibrated hydrograph.

Error	Algorithm	Efficiency		RMS Error (10^{-6})	
		Mean	Standard Deviation	Mean	Standard Deviation
Uncorrelated	MDG	0.332	0.050	3.45	0.95
	MAG	0.963	0.021	0.81	0.61
	MDN	0.771	0.108	2.02	1.39
	TPP	0.024	0.032	4.17	0.75
	FCN	0.471	0.086	3.07	1.24
	FDN	0.866	0.061	1.55	1.05
	ENU	0.940	0.044	1.03	0.89
	OODS	0.909	0.057	1.27	0.75
Correlated	MDG	0.773	0.047	2.01	0.91
	MAG	0.854	0.043	1.61	0.88
	MDN	0.891	0.165	1.39	1.71
	TPP	0.718	0.093	2.24	1.29
	FCN	0.951	0.044	0.93	0.88
	FDN	0.991	0.013	0.41	0.49
	ENU	0.990	0.014	0.42	0.50
	OODS	0.990	0.015	0.41	0.49

method. For the MDG calibration with uncorrelated error this method resulted in a *negative* efficiency – indicating that even a straight line would have outperformed it. The poor performance of the TPP method is most likely due to its poor definition of drainage networks, and corresponding generation of strange topographic index distributions.

In addition to a quantitative analysis based on the efficiency and rms, the ability of TOPMODEL to produce realistic hydrographs can also be investigated qualitatively by examining the output hydrographs. Figures 6.2 and 6.2 show the mean hydrographs estimated by TOPMODEL for all eight algorithms using the MDG and ENU calibrations, respectively. These results are for the addition of uncorrelated error to the DEM. In comparing the two calibrations it can be seen that, in general, the ENU calibration produces hydrographs for the eight algorithms that are more similar. This is because the topographic distribution used for ENU calibration is more representative of the topographic distributions created by the eight algorithms. This is, however, not the same as saying that the ENU calibration creates a distribution that is more correct, as it has already been shown that the ENU method does not produce a very definable drainage network. It is, therefore, unlikely that the method – or the others not based on the steepest neighbour principle – produces a topographic distribution that accurately describes the watershed.

To avoid the presentation of an excess number of similar graphs, the hydrographs for the correlated DEM error are not provided. The only difference between the hydrographs created using uncorrelated DEM error and those created using correlated DEM error is that the correlated error hydrographs fit the calibrated hydrographs better. As a result there is less of a difference between the algorithms' hydrographs.
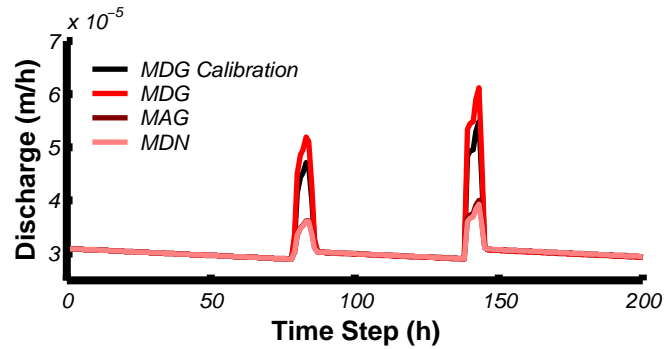
(a) Steepest Neighbour Algorithms
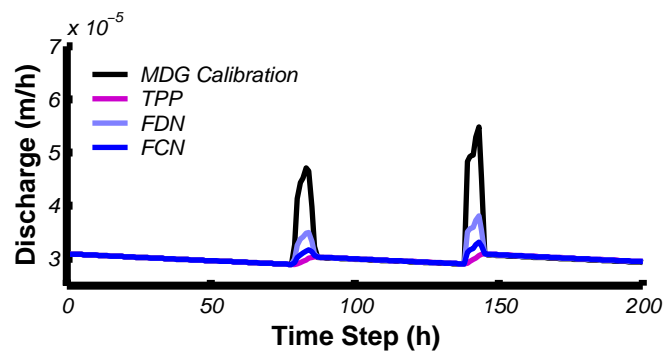
(b) Three and Four Neighbour Algorithms
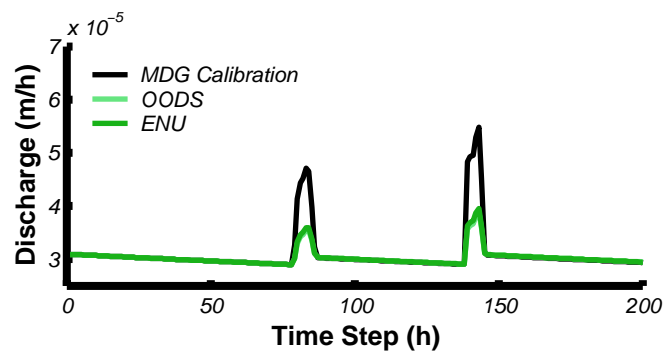
(c) Eight Neighbour Algorithms

Figure 6.11: Mean TOPMODEL estimated hydrographs for the eight slope and aspect algorithms using uncorrelated error and the MDG calibration. The calibrated stream hydrograph is provided for comparison.

(a) Steepest Neighbour Algorithms

(b) Three and Four Neighbour Algorithms

(c) Eight Neighbour Algorithms

Figure 6.12: Mean TOPMODEL estimated hydrographs for the eight slope and aspect algorithms using uncorrelated error and the ENU calibration. The calibrated stream hydrograph is provided for comparison.

Two of the more important characteristics of a hydrograph are the times to and heights of the discharge peaks following rain events. In the 200 hour time series studied here there were two rain events. The mean and standard deviation of the peak values for MDG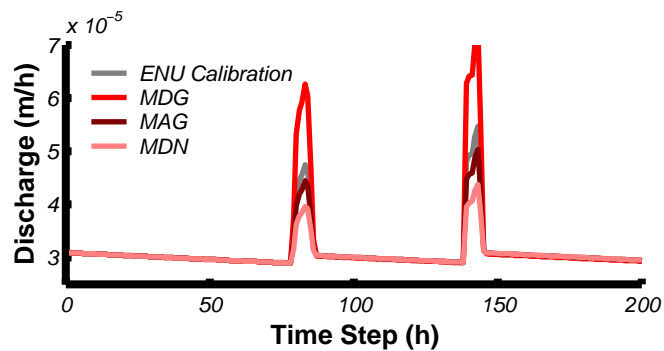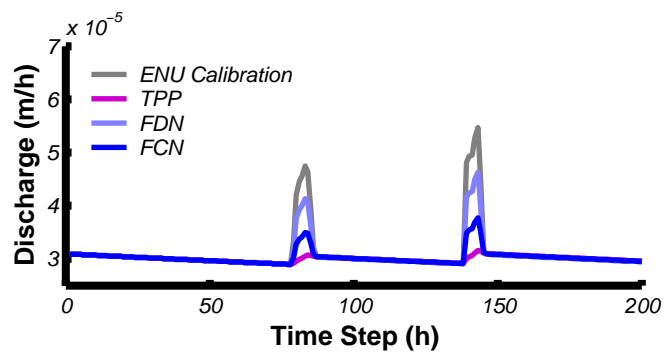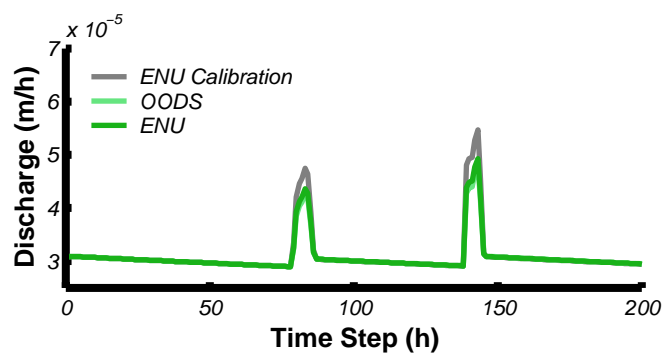 and ENU are available in Tables 6.8 and 6.9,respectively. For each calibration method there is little to no difference between the times to the discharge peaks for most of the eight algorithms or error types. This is especially true for ENU calibration. There is however, one notable exception to this, the TPP algorithm. This algorithm produces hydrographs that are almost completely flat, making the determination of the peak location difficult at times. Again, this poor result is because the TPP algorithm does not generate any sort of drainage network. Therefore, the discharge produced by TOPMODEL for this algorithm is similar to the discharge that would be produced from a relativey flat area. The difference in the peak heights between algorithms can be seen in Figures 6.2 and 6.2.

Regardless of the algorithm, calibration method, or type of DEM error, the standard deviations of the peak values are very small. This is particularly true for the ENU calibration, where, in some cases, the standard deviation is virtually zero. Even the standard deviations for MDG calibration are, however, fairly insignificant. As expected the smallest standard deviations occur for the algorithms used to calibrate the model. From these results it appears that DEM error does not have a significant effect on TOPMODEL's hydrograph estimation.

One thing that stands out when examining the results for TOPMODEL is the large differences between hydrographs for different algorithms. The magnitude of these differences is somewhat surprising considering all the data is for the same watershed and rain event. For a given set of calibrated parameters the only difference in the

Table 6.8: Characteristics of the hydrographs produced using MDG calibration.

Error/Algorithm		Time to Peak(h)				Discharge (10^{-5}m/h)			
		Peak 1		Peak 2		Peak 1		Peak 2	
		Mean	Standard Deviation	Mean	Standard Deviation	Mean	Standard Deviation	Mean	Standard Deviation
Uncorrelated	MDG	6.11	0.00	4.54	0.00	5.19	0.04	6.13	0.06
	MAG	6.92	0.39	4.54	0.00	3.62	0.07	3.67	0.13
	MDN	6.16	0.21	4.54	0.00	3.61	0.10	3.86	0.23
	TPP	9.05	0.26	6.40	0.35	3.04	0.01	3.04	0.01
	FCN	7.12	0.09	4.54	0.00	3.18	0.05	3.24	0.05
	FDN	7.10	0.13	4.54	0.00	3.50	0.07	3.53	0.06
	ENU	7.01	0.31	4.54	0.00	3.60	0.08	3.63	0.11
	OODS	7.04	0.26	4.54	0.00	3.55	0.08	3.59	0.11
Correlated	MDG	6.11	0.00	4.54	0.00	4.62	0.06	5.35	0.08
	MAG	6.11	0.00	4.54	0.00	4.40	0.08	5.07	0.11
	MDN	6.22	0.32	4.54	0.00	4.15	0.28	4.67	0.48
	TPP	7.11	0.00	4.54	0.00	3.23	0.06	3.30	0.06
	FCN	7.06	0.23	4.54	0.00	3.57	0.08	3.60	0.08
	FDN	6.39	0.45	4.54	0.00	3.78	0.09	3.94	0.29
	ENU	6.38	0.44	4.54	0.00	3.78	0.08	3.95	0.29
	OODS	6.35	0.43	4.54	0.00	3.78	0.08	3.97	0.29

Table 6.9: Characteristics of the hydrographs produced using ENU calibration.

Error/Algorithm		Time to Peak(h)				Discharge (10^{-5} m/h)			
		Peak 1		Peak 2		Peak 1		Peak 2	
		Mean	Standard Deviation	Mean	Standard Deviation	Mean	Standard Deviation	Mean	Standard Deviation
Uncorrelated	MDG	6.11	0.00	4.54	0.00	6.27	0.06	7.30	0.07
	MAG	6.11	0.00	4.54	0.00	4.45	0.10	5.03	0.12
	MDN	6.11	0.00	4.54	0.00	3.97	0.21	4.38	0.29
	TPP	7.55	0.56	4.92	0.49	3.08	0.02	3.08	0.04
	FCN	6.19	0.27	4.54	0.00	3.50	0.10	3.56	0.17
	FDN	6.11	0.00	4.54	0.00	4.14	0.14	4.64	0.19
	ENU	6.11	0.00	4.54	0.00	4.37	0.16	4.93	0.21
	OODS	6.11	0.00	4.54	0.00	4.26	0.17	4.80	0.21
Correlated	MDG	6.11	0.00	4.54	0.00	5.63	0.09	6.53	0.11
	MAG	6.11	0.00	4.54	0.00	5.55	.010	6.32	0.13
	MDN	6.11	0.08	4.54	0.00	5.10	0.48	5.91	0.63
	TPP	6.11	0.00	4.54	0.00	3.82	0.16	4.04	0.38
	FCN	6.11	0.00	4.54	0.00	4.40	0.18	5.03	0.23
	FDN	6.11	0.00	4.54	0.00	4.81	0.16	5.55	0.21
	ENU	6.11	0.00	4.54	0.00	4.80	0.17	5.54	0.22
	OODS	6.11	0.00	4.54	0.00	4.79	0.17	5.53	0.22

input data for TOPMODEL is the topographic distribution. From the models perspective, using topographic distributions with different distribution statistics (min, max, mean, standard deviation and skew) essentially describes different watersheds. With this understanding, the apparent extreme differences between algorithms become more understandable.

In a study done by Wolock and Price (1994), it was found that the hydrographs predicted by TOPMODEL were very sensitive to the mean of the input topographic distribution. The higher the mean, the greater the ground saturation and, hence ,the greater the amount of overland flow during rain events. In this study, TOPMODEL was found to be more sensitive to the right skewness of the topographic distribution than the mean. The higher the skew produced by an algorithm, the higher the peak discharge. The reason the skewness had more of an impact then the mean is probably related to the dryness of the watershed. Since the watershed was fairly dry, and, since the rain event was not very large, not much of the watershed was ever saturated. Hence, it was the tail of the topographic index distribution that was more significant in determining the amount of saturation. By comparing skew values and hydrographs it can be seen that similar hydrographs are produced by algorithms with similarly skewed topographic distributions.

The objective of this study was to examine the effect of uncorrelated and correlated DEM error on the output from TOPMODEL. Therefore, the standard deviations in the results over the 500 realisations should be investigated, and not the differences between the mean values of the eight algorithms. In any case, the difference between algorithms can essentially be 'calibrated out' with a re-calibration of TOPMODEL. Therefore, looking at the variations in results for each algorithm, especially those

in the algorithms that were used for calibration, it appears that DEM error – either uncorrelated or correlated – has little impact on TOPMODEL's results. That is, the output from TOPMODEL does not appear to be sensitive to DEM error for the watershed investigated in this study.

Chapter 7

Conclusions

This research studied the effect of uncorrelated and correlated DEM error on the determination of four topographic parameters: slope, aspect, upslope area and topographic index. In addition, the effect of DEM error on the distributed hydrological model TOPMODEL was also investigated. For both investigations the objective was to determine which slope and aspect algorithms had the greatest sensitivity to DEM error.

Conclusions that can be made from the results presented in the previous chapter are as follows:

- **Correlated versus uncorrelated DEM error:** The error in most topographic parameters was significantly smaller in the presence of correlated DEM error than in the presence of uncorrelated DEM error. This was true for the slope, upslope area and topographic index. The exception to this was the aspect, where there was little difference in error between uncorrelated and correlated error.

- **Slope:** The more neighbours used in a slope algorithm, the less sensitive the algorithm is to DEM error. This is true both for those algorithms based on the steepest neighbour principle, and those algorithms that use a fixed number of neighbours. Furthermore, the former category of algorithms was, in general, more susceptible to error than the latter category. When the eight algorithms are ranked from highest to lowest amount of error the result is as follows: TPP, MDG, MAG, FCN, MDN, FDN, OODS and ENU.

  For the two algorithms studied in detail (ENU and MDG), the sensitivity of the slope error was smallest in regions of low slope. Outside of these regions the ENU algorithm had an error sensitivity that was fairly uniform. In contrast, the error sensitivity of the MDG method was dependant upon the value of slope. It is believed that such results are representative of the two different categories of slope algorithms, and that, compared to those algorithms that use a fixed number of neighbours, the error sensitivity of algorithms based on the steepest neighbour principle is, in general, more dependant upon the slope value.

- **Aspect:** Aspect error is essentially equal for all eight slope and aspect algorithms studied. This error has a value of approximately $45°$, which represents an aspect displacement of one grid cell. The variation in the magnitude of aspect error across the watershed is not dependent on the aspect value itself. Rather, it is related to the value of slope. In particular, areas of low slope tend to correspond to areas of high aspect error.

- **Upslope area:** For the upslope area derived from slope and aspect algorithms based on the steepest neighbour principle, it was observed that the more per-

missive the choice of neighbour (or neighbours), the less sensitive the upslope area was to DEM error. Or, equivalently, the smaller the dependance on a single downhill neighbour, the smaller the error sensitivity. Conversely, for those algorithms not based on the steepest neighbour, the error sensitivity of upslope area increases with an increase in the number of neighbours used in the algorithm.

The error sensitivity of the upslope area is greatest for those algorithms that produce distinctly defined drainage networks. This is because it is along the drainage networks that the largest upslope area errors occur. The steepest neighbour algorithms are the most adept at producing well-defined networks, and consequently have the greatest error sensitivity. The eight algorithms can be ranked from highest to lowest amount of upslope area error as a result of DEM error as follows: MDG, MAG, MDN, OODS, ENU, FDN, FCN and TPP.

- **Topographic index:** Errors in the topographic index are largest for the algorithms based on the steepest neighbour principle. Within this category, a similar error pattern is observed as was seen for both the slope and upslope area: the more permissive the choice of neighbour (or neighbours), the smaller the error sensitivity. The topographic index error pattern for the algorithms that use a fixed number of neighbours is, again, similar to that observed for slope: the more neighbours used in an algorithm, the less sensitive the result is to DEM error. Errors in topographic index are greatest along the drainage network and in areas of low slope. As discussed previously, however, the steepest-neighbour algorithms produce the most clearly defined drainage networks, and consequently have a greater overall error. Thus, when the eight algorithms can

be ranked from largest to smallest amounts of error, the steepest neighbour algorithms come out on top: MDG, MDN, MAG, TPP, FCN, OODS, FDN and ENU.

- **TOPMODEL:** For the watershed investigated in this study, the output from TOPMODEL does not appear to be sensitive to DEM error. This is true for any of the slope and aspect algorithms used to generate the topographic index distribution, and is reflected in the very low standard deviations in the times-to-peak and peak discharge values. The values themselves are, however, sensitive to the choice of algorithm – particularly the peak discharge. This is because each slope and aspect algorithm calculates the topographic index in a different way, and therefore the topographic index distributions are all slightly different. From the model's perspective, topographic distributions with different statistics are, essentially, different watersheds altogether, and hence give different discharge results.

Attention should be brought to the fact that this research was performed on a single watershed with a specific amount of elevation error and error correlation. While it is felt that the conclusions from this research are valid for a wide variety of watersheds with a range of elevation error magnitudes and correlations, care should be taken when applying these conclusions too strictly. Before these conclusions can be globally applied, research should be done into the effects of increased and decreased amounts of DEM error, different types of error correlation, as well the effects on watersheds from different types of terrain.

Bibliography

Ackermann, F. (1992). High-quality digital terrain models - the SCOP program and derived products. *EARSeL Advances in Remote Sensing*, 1(3):122–128.

Band, L. E. (1986). Topographic partition of watersheds wtih digital elevation models. *Water Resources Research*, 22(1):15–24.

Beven, K. J. and Kirkby, M. J. (1979). A physically based, variable contributing area model of basin hydrology. *Hydrological Sciences Bulletin*, 24(1):43–69.

Bruneau, P., Gascuel-Odoux, C., Robin, P., Ph., M., and Beven, K. (1995). Sesnistivity to space and time resolution of a hydrological model using digital elevation data. *Hydrological Processes*, 9:69–81.

Costa-Cabral, M. C. and Burges, S. J. (1994). Digial elevation model networks (DEMON): a model of flow over hillslopes for computation of contributing and dispersal areas. *Water Resources Research*, 30(6):1681–1692.

Dozier, J. and Strahler, A. H. (1983). Ground invetigations in support of remote sensing. In Colwell, R. N. and Simonett, D. S., editors, *Manual of Remote Sensing*, volume 1, chapter 23, pages 959–986. American Society of Photogrammetry, Virginia, 2 edition.

Evans, I. S. (1980). An integrated system of terrain anylysis and slope mapping. *Zeitschrift für Geomorphologie N. F.*, Supplementband 36:274–295.

Eyton, J. R. (1991). Rate-of-change maps. *Cartography and Geographic Information Systems*, 18(2):87–103.

Fairfield, J. and Leymarie, P. (1991). Drainage networks from grid digital elevation models. *Warer Resources Research*, 27(5):709–717.

Fisher, P. F. (1991a). First experiments in viewshed uncertainty: The accuracy of the viewshed area. *Photogrammetric Engineering and Remote Sensing*, 57(10):1321–1327.

Fisher, P. F. (1991b). Modelling soil map-unit inclusions by Monte Carlo simulation. *International Journal of Geographical Information Systems*, 5(2):193–208.

Franchini, M., Wendling, J., Obled, C., and Todini, E. (1996). Physical interpretation and sensitivity analysis of the TOPMODEL. *Journal of Hydrology*, 175:293–338.

Freeman, T. G. (1991). Calculating catchment area with divergent flow based on a regular grid. *Computers and Geoscience*, 17(3):413–422.

Gallant, J. C. and Wilson, J. P. (2000). Primary topographic attributes. In Wilson, J. P. and Gallant, J. C., editors, *Terrain Analysis: Principles and Applications*, chapter 3, pages 51–85. John Wiley & Sons, Inc., New York.

Guth, P. L. (1995). Slope and aspect calculations on gridded digital elevation models: Examples from a geomorphometric toolbox for personal computers. *Zeitschrift für Geomorphologie N. F.*, Supplementband 101:31–52.

Heuvelink, G. B. M. (1998). *Error Propagation in Environmental Modelling with GIS*. Taylor & Francis, London.

Hodgson, M. E. (1995). What cell size does the computed slope/aspect angle represent. *Photogrammetric Engineering and Remote Sensing*, 61(5):513–517.

Hoffer, R. M., Fleming, M. D., Bartolucci, L. A., and Davis, S. M. amd Nelson, R. F. (1979). Digital processing of landsat MSS and topographic data to improve capabilities for computerized mapping of forest cover types. *LARS Technical Report 011579. Laboratory for Applications of Remote Sensing, Purdue University, West Lafayette, Indiana*.

Holmes, K. W., Chadwick, O. A., and Kyriakidis, P. C. (2000). Error in a USGS 30-meter digital elevation model and its impact on terrain modeling. *Journal of Hydrology*, 233:154–173.

Horn, B. K. P. (1981). Hill shading and the reflectance map. *Proceedings of the IEEE*, 69(1):14–47.

Hutchinson, M. F. (1989). A new procedure for gridding elevation and stream line data with automatic removal of spurious pits. *Journal of Hydrology*, 106:211–232.

Jenson, S. K. and Dominque, J. O. (1988). Extracting topographic structure from digital elevation data for geographic information system analysis. *Photogrammetric Engineering and Remote Sensing*, 54(11):1593–1600.

Jones, K. H. (1998). A comparison of algorithms used to compute hill slope as a property of the DEM. *Computers and Geosciences*, 24(4):315–323.

Lee, J., Snyder, P. K., and Fisher, P. F. (1992). Modeling the effect of data errors on feature extraction from digital elevation models. *Photogrammetric Engineering and Remote Sensing*, 58(10):1461–1467.

Martz, L. W. and de Jong, E. (1988). CATCH: a FORTRAN program for measuring catchment area from digital elevation models. *Computers and Geoscience*, 14(5):627–640.

Monteith, J. (1965). Evaporation and the environment. In *The State and Movement of Water in Living Organisms*, pages 205–234. XIXth Symposium Soc. for Exp. Biol., Swansea, Cambridge University press.

Nash, J. E. and Sutcliffe, J. V. (1970). River flow forecasting through conceptual models part I - a discussion of principles. *Journal of Hydrology*, 10:282–290.

O'Callaghan, J. F. and Mark, D. M. (1984). The extraction of drainage networks form digital elevation data. *Computer Vision, Graphics, and Image Processing*, 28:323–344.

O'Neill, M. P. and Mark, D. M. (1987). On the frequency ditribution of land slope. *Earth Surface Processes and Landforms*, 12:127–136.

Onorati, M., Poscolieri, R., Ventura, R., Chiarini, V., and Crucillà (1992). The digital elevation model of Italy for geomorphology and structural geology. *Catena*, 19:147–178.

Papo, H. B. and Gelbman, E. (1984). Digital terrain models for slopes and curvatures. *Photogrammetric Engineering and Remote Sensing*, 50(6):695–701.

Quinn, P., K., B., Chevallier, P., and Planchon, O. (1991). The prediction of hillslope flow paths for distributed hydrological modelling using digital terrain models. *Hydrological Processes*, 5:59–79.

Quinn, P. F., Beven, K. J., and Lamb, R. (1995). The $\ln(a/\tan\beta)$ index: How to calculate it and how to use it within the TOPMODEL framework. *Hydrological Processes*, 9:161–182.

Ritter, P. (1987). A vector-based slope and aspect generation algorithm. *Photogrammetric Engineering and Remote Sensing*, 53(8):1109–1111.

Sharpnack, D. A. and Akin, G. (1969). An algorithm for computing slope and aspect from elevations. *Photogrammeteric Engineering*, 35(3):247–248.

Skidmore, A. K. (1989). A comparison of techniques for calculating gradient and aspect from a gridded digital elevation model. *Internation Journal of Geographical Information Systems*, 3(4):323–334.

Tarboton, D. G. (1997). A new method for the determination of flow directions and upslope areas in grid digital elevation models. *Water Resources Research*, 33(2):309–319.

Tribe, A. (1992). Automated recognition of valley lines and drainage networks from grid digital elevation models: a review and a new method. *Journal of Hydrology*, 139:263–293.

Unwin, D. (1981). *Introductory Spatial Analysis*. Methuen, New York. pp212.

Veregin, H. (1997). The effects of vertical error in digital elevation models on teh determination of flow-path direction. *Cartography and Geographic Information Systems*, 24(2):67–79.

Wolock, D. M. and McCable Jr., G. J. (1995). Comparision of single and multiple flow direction algorithms for computing topographic parameters in TOPMODEL. *Water Resources Research*, 31(5):1315–1324.

Wolock, David, M. and Price, C. V. (1994). Effects of digital elevation model map scale and data resolution on a topography-based watershed model. *Water Resources Research*, 30(11):3041–3052.

Zevenbergen, L. W. and Thorne, C. R. (1987). Quantitative analysis of land surface topography. *Earth Surface Processes and Landforms*, 12:47–56.